

A&A manuscript no.
(will be inserted by hand later)

Your thesaurus codes are:
08(08.01.2;08.03.3;08.06.3;08.16.2;03.20.8)

On the Ages of Exoplanet Host Stars [★]

Carlos Saffe^{**}, Mercedes Gómez and Carolina Chavero^{***,†}

Observatorio Astronómico de Córdoba, Laprida 854, 5000 Córdoba, Argentina
email: saffe@oac.uncor.edu, mercedes@oac.uncor.edu, carolina@oac.uncor.edu

Received Month XX, 200X; accepted Month XX, 200X

Abstract. We obtained spectra, covering the CaII H and K region, for 49 exoplanet host (EH) stars, observable from the southern hemisphere. We measured the chromospheric activity index, R'_{HK} . We compiled previously published values of this index for the observed objects as well as the remaining EH stars in an effort to better smooth temporal variations and derive a more representative value of the average chromospheric activity for each object. We used the average index to obtain ages for the group of EH stars. In addition we applied other methods, such as: Isochrone, lithium abundance, metallicity and transverse velocity dispersions, to compare with the chromospheric results. The kinematic method is a less reliable age estimator because EH stars lie red-ward of Parenago's discontinuity in the transverse velocity dispersion vs dereddened B–V diagram. The chromospheric and isochrone techniques give median ages of 5.2 and 7.4 Gyr, respectively, with a dispersion of ~ 4 Gyr. The median age of F and G EH stars derived by the isochrone technique is ~ 1 –2 Gyr older than that of identical spectral type nearby stars not known to be associated with planets. However, the dispersion in both cases is large, about ~ 2 –4 Gyr. We searched for correlations between the chromospheric and isochrone ages and L_{IR}/L_{\odot} (the excess over the stellar luminosity) and the metallicity of the EH stars. No clear tendency is found in the first case, whereas the metallicity dispersion seems to slightly increase with age.

Key words: Stars: activity, chromospheres, fundamental parameters, planetary systems - Techniques: spectroscopy

Send offprint requests to: C. Saffe

^{*} Based on observations collected at the Complejo Astronómico El Leoncito (CASLEO) operated under agreement between the Consejo Nacional de Investigaciones Científicas y Técnicas de la República Argentina and the National Universities of La Plata, Córdoba and San Juan.

^{**} On a fellowship from CONICET, Argentina.

^{***} Also at the Facultad de Matemática, Astronomía y Física de la Universidad Nacional de Córdoba, Argentina.

[†] Present address: Observatório Nacional, Rua General José Cristiano 77, São Cristóvão, 20921-400 Rio de Janeiro, Brasil.

1. Introduction

During the last decade, the detection of more than one hundred nearby solar-type stars associated with likely single or multiple planetary mass companions (Mayor & Queloz 1995; Butler et al. 1999) has given rise to new interest in the study of these relatively bright stellar objects (see, for example, Reid 2002).

At the present time, most of the known EH stars have been detected by means of the Doppler technique and are, in general, among the less chromospherically active and slow-rotation solar-type stars. The reason for this selection effect is that chromospherically active stars have stellar surface features, such as convective inhomogeneities or magnetic spots that may induce intrinsic stellar radial-velocity "jitter" indistinguishable from the orbital motion of the star around the center of mass of the star and planet system (Saar & Donahue 1997; Saar et al. 1998). These effects may inhibit or even provide false detections (Walker et al. 1992; Santos et al. 2000b; Queloz et al. 2001; Paulson et al. 2002, 2004).

It is well established that the Exoplanet Host (EH) sample, on average, is metal-rich compared to solar neighborhood field stars not known to have planets, detectable by means of high precision radial velocity measurements (Gonzalez 1997; Laughlin & Adams 1997; Gonzalez 1998; Gonzalez et al. 2001a; Santos et al. 2000a, 2001, 2004b).

Suchkov & Schultz (2001) analyzed nine F-type stars associated with exoplanets and determined their ages by using different estimators, such as: metallicity, Hipparcos variability, brightness anomaly and location in the color-magnitude diagram in relation to field F stars and the Hyades. They concluded that the 9 analyzed stars have ages similar to Hyades (~ 0.7 Gyr) and thus are significantly younger than F field stars. The age may thus be a parameter that can help in selecting candidate EH stars. Moreover, the age is a fundamental parameter that it is worth while exploring.

In this contribution we present spectra for 49 EH stars observed from the southern hemisphere and apply the stellar chromospheric activity to obtain their ages. From the literature we derive the chromospheric index, R'_{HK} , for the remaining stars with no spectra reported in this contribution. We compare the "chromospheric" age determinations with those calculated us-

ing other methods, such as: Isochrones, lithium and metallicity abundances, and space velocity dispersions. We confront the EH stars ages with those of nearby stars of similar characteristics not known to be associated with planets. We search for correlations between the age and physical parameters of the EH stars such as, the L_{IR}/L_* (the excess over the stellar luminosity) and the metallicity.

In Section 2 we present our observations and in Section 3 we apply the CaII H, K core emissions to measure the chromospheric activity and to derive ages. The other age estimators are described and discussed in Sections 4. We compare the ages of the EH stars with those of solar neighborhood stars of similar spectral types not associated with planets in Section 5. Finally, we search for correlations of physical properties of the stars with age in Section 6. We conclude with a brief summary in Section 7.

2. Observations and data reduction

We observed 49 southern hemisphere EH stars from the California and Carnegie Planet Search¹ and the Geneva Observatory Planet Search² lists. These compilations basically include 138 EH stars up to 06/25/2005, including 157 exoplanets and 14 multiple systems. 131 EH stars have been detected by Doppler spectroscopy and only 7 by photometry. The likely planetary companions have masses such that $M \sin i < 17 M_{\text{JUP}}$. The 49 stars we observed have distances between 10 and 94 pc and spectral types F, G, and K (6, 34, and 9 objects, respectively), as specified in the Hipparcos database.

We carried out the observations on September 20–22 2003 and March 28–31 2004, at the Complejo Astronomico El Leoncito (CASLEO, San Juan - Argentina) with the REOSC spectrograph attached to the Jorge Sahade 2.15-m telescope. The REOSC has a TEK 1024 × 1024 back illuminated detector, with a pixel size of 24 × 24 μm , and it was employed in single dispersion mode. We used a 1200 l/mm grating (0.75 $\text{\AA}/\text{pix}$) centered at 3950 \AA to cover the spectral range 3500–4200 \AA , including the CaII H and K lines, at 3968 and 3933 \AA , respectively. We selected a 250 μm ($\sim 1''$) wide slit. Several chromospheric "standards" were observed during both observing runs. The integration times varied between 1 and 10 minutes, depending on the sources brightness. A pair of CuNeAr lamp spectra was taken for each object. To reduce the spectra and measure CaII H and K lines fluxes we used IRAF³.

The spectra were extracted using the NOAO task *apall* with an aperture of 5 pixel radius. A sky subtraction was carried out by fitting a polynomial to the regions on either side of the aperture. A non linear low order fit to the lines in the CuNeAr lamp was used to wavelength calibrate the spectra. Typical RMS for the wavelength solution is 0.22. The *sbands* task was used to measure the fluxes in the CaII lines cores.

3. Age derivation from the chromospheric activity

The stellar chromospheric emission (CE) as measured by the core emission in the CaII H and K absorption lines, is related to both the spectral type (Wilson 1970; Baliunas et al. 1995a) and the rotational velocity of the central star (see, for example, Wilson 1963; Skumanich 1972; Barry et al. 1987; Eggen 1990; Soderblom et al. 1991). Late spectral type main-sequence stars have larger chromospheric activity than early type objects (Wilson 1970). As the object ages, it slows down its rotation and diminishes the level of CE (Wilson 1963; Noyes et al. 1984; Rocha-Pinto & Maciel 1998). In this sense, the CE provides an indication of the stellar age for a given spectral type.

The chromospheric activity is quantified by the S and R'_{HK} indexes (e.g. Vaughan et al. 1978; Baliunas et al. 1995a; Vaughan & Preston 1980; Baliunas et al. 1995b; Soderblom et al. 1991; Henry et al. 1996). The S index is defined by the sum of fluxes within two 1- \AA -width bands centered on the CaII H ($\lambda 3968 \text{\AA}$) and K ($\lambda 3933 \text{\AA}$) lines. Then the combined flux is normalized to the pseudo-continuum level as measured by two equidistant windows of 20- \AA -width each, on either side of the CaII lines. According to this definition it is not necessary to flux calibrate the spectra as the index definition involved relative measurements.

The R'_{HK} index introduces two modifications to the S index: 1) a B–V color correction,

$$R_{\text{HK}} = C(B - V) S, \quad (1)$$

and 2) the subtraction of the photospheric contribution, R_{PHOT} :

$$R'_{\text{HK}} = R_{\text{HK}} - R_{\text{PHOT}}. \quad (2)$$

We refer to the paper of Noyes et al. (1984) for a detailed description of the derivation of both $C(B-V)$ and R_{PHOT} .

To determine S and R'_{HK} for the observed stars we basically adopted the procedure of Henry et al. (1996). We define the S_{CASLEO} index analogous to Equation 1 and transform this index to the Mount Wilson four spectrophotometric bands (Vaughan et al. 1978) by means of the standard stars measurements. Specifically, in the determination of S_{CASLEO} we used two 3- \AA -width bands centered on the CaII lines and two 20- \AA -width pseudo-continuum windows located on either side of the H and K lines. In Table 1 we list the standard stars observed, selected from among those with more than 100 observations at Mount Wilson. We include the S and R'_{HK} indexes corresponding to the Mount Wilson and the CASLEO measurements.

To estimate the errors in our determinations of S_{CASLEO} for the observed objects we displaced the on-line windows half a pixel on either direction, re-calculated the index in each case and then compared with the original measurements. In this manner we estimate an error of ~ 0.005 in S_{CASLEO} due to misplacements of the on-line windows. Translated to age, an error of ~ 0.005 corresponds to ~ 0.4 Gyr for a 5 Gyr old star. In this estimation we used the Donahue (1993)'s calibration.

Figure 1, upper panel, shows the S_{CASLEO} vs S_{MW} indexes plot corresponding to each observing run. We used a second

¹ <http://exoplanets.org>

² <http://obswww.unige.ch/exoplanets>

³ IRAF is distributed by the National Optical Astronomy Observatory, which is operated by the Association of Universities for Research in Astronomy, Inc. under contract to the National Science Foundation.

Table 1. Chromospheric standard stars measured at the CASLEO.

Star	S_{MW}	$\text{Log } R'_{MW}$	S_{CASLEO}	$\text{Log } R'_{CASLEO}$
September 2003				
HD 3443 AB	0.1823	-4.907	0.3706	-5.077
HD 3795	0.1557	-5.038	0.3443	-5.146
HD 9562	0.1365	-5.174	0.3526	-5.124
HD 10700	0.1712	-4.959	0.3739	-5.066
HD 11131	0.3355	-4.428	0.4582	-4.580
HD 16673	0.2151	-4.662	0.4307	-4.671
HD 17925	0.6478	-4.314	0.5870	-4.263
HD 22049	0.4919	-4.458	0.5129	-4.536
HD 30495	0.2973	-4.510	0.4431	-4.648
HD 38393	0.1514	-4.941	0.3842	-4.946
HD 152391	0.3867	-4.461	0.5053	-4.432
HD 158614 AB	0.1581	-5.028	0.3708	-5.076
March 2004				
HD 23249	0.1374	-5.184	0.2754	-5.037
HD 30495	0.2973	-4.510	0.4007	-4.414
HD 38392	0.5314	-4.497	0.4811	-4.389
HD 38393	0.1514	-4.941	0.3385	-5.004
HD 45067	0.1409	-5.092	0.3178	-5.094
HD 76151	0.2422	-4.670	0.3712	-4.700
HD 81809 AB	0.1720	-4.923	0.3135	-5.089
HD 158614	0.1581	-5.028	0.3138	-4.944

order fit to reproduce the data point (the continuous line) and derive the following relations:

$$S_{MW} = 4.1109 S_{CASLEO}^2 - 1.6104 S_{CASLEO} + 0.1966 \quad (3)$$

$$S_{MW} = 8.7210 S_{CASLEO}^2 - 4.6370 S_{CASLEO} + 0.7476, \quad (4)$$

for the September 2003 and March 2004 observing runs, respectively. These relations are strictly valid for $0.27 < S_{CASLEO} < 0.59$ ($0.14 < S_{MW} < 0.65$) September 2003 and $0.27 < S_{CASLEO} < 0.48$ ($0.14 < S_{MW} < 0.53$) March 2004. HD 162020, one of the most chromospheric active EH stars ($S_{CASLEO} = 1.11$), is the only object in our sample outside the ranges of Equations 3 and 4. In this case we extrapolated these relations to include this object in our analysis.

Figure 1, lower panel, compares the $\text{Log } R'_{HK}$ values corresponding to CASLEO and Mount Wilson for the standard stars measurements (see also Table 1). We derived an uncertainty of ~ 0.05 dex for the CASLEO calibration with respect to the Mount Wilson relation. This value mainly reflects the fact that the CE of the stars varies over time. Systematic errors in the CASLEO calibration with respect to the Mount Wilson standard are likely to be much smaller than this amount. An uncertainty of ~ 0.05 dex, similar to those derived by Henry et al. (1996) or Strassmeier et al. (2000), corresponds to an age difference of ~ 1.5 Gyr for a 5 Gyr old star, using the Donahue (1993)'s calibration.

The CE varies with time, having short and long periodic and non-periodic variations (Noyes et al. 1984; Baliunas et al. 1995a,b). The use of instantaneous values of the indexes S and $\text{Log } R'_{HK}$ (i.e., corresponding to a given epoch of observation) can induce to erroneous age estimations. For example, in the

case of the Sun the R'_{HK} varied from -4.75 to -5.10 during the "Maunder Minimum" (~ 1650 , ~ 1890), corresponding to ages of 8.0 and 2.2 Gyr, respectively. Although this represents an extreme variation (at present, only certainly detected for the Sun), it cautions on the applicability of individual values of the CE index. For this reason it is more appropriate to use the temporal average, $\langle R'_{HK} \rangle$, to estimate the age.

We have extensively searched the literature for previous determinations of the index R'_{HK} for all the stars observed at the CASLEO and the rest of the sample of EH stars. Table 2 shows a one-sample page of our compilation as well as the data reported in this contribution. The complete table is available in electronic format. As the data are published in different manners, for example individual or average observations for each observing run, we have also indicated the type of data used in the final average in Table 2.

In Table 3 we list the $\text{Log } R'_{HK}$ values derived from the CASLEO data only, the average compiled from the literature, $\langle \text{Log } R'_{HK} \text{ without CASLEO} \rangle$, and the final average including our CASLEO measurements, $\langle \text{Log } R'_{HK} \text{ with CASLEO} \rangle$. The average difference between the indexes with and without the data reported in this contribution is ~ 0.107 . Three stars in the sample, HD 19994, HD 169830 and HD 216437, show average differences significantly larger, 0.569, 0.381 and 0.222, respectively. In Table 4 we list the $\langle \text{Log } R'_{HK} \rangle$ obtained from the literature for the objects not observed at the CASLEO.

To derive the "chromospheric age" for the EH objects we applied the calibrations of Donahue (1993), hereafter D93, and Rocha-Pinto & Maciel (1998), hereafter RPM98. The latter relation includes a correction in the age derivation due to the stellar metallicity. The derived values are listed in columns 5

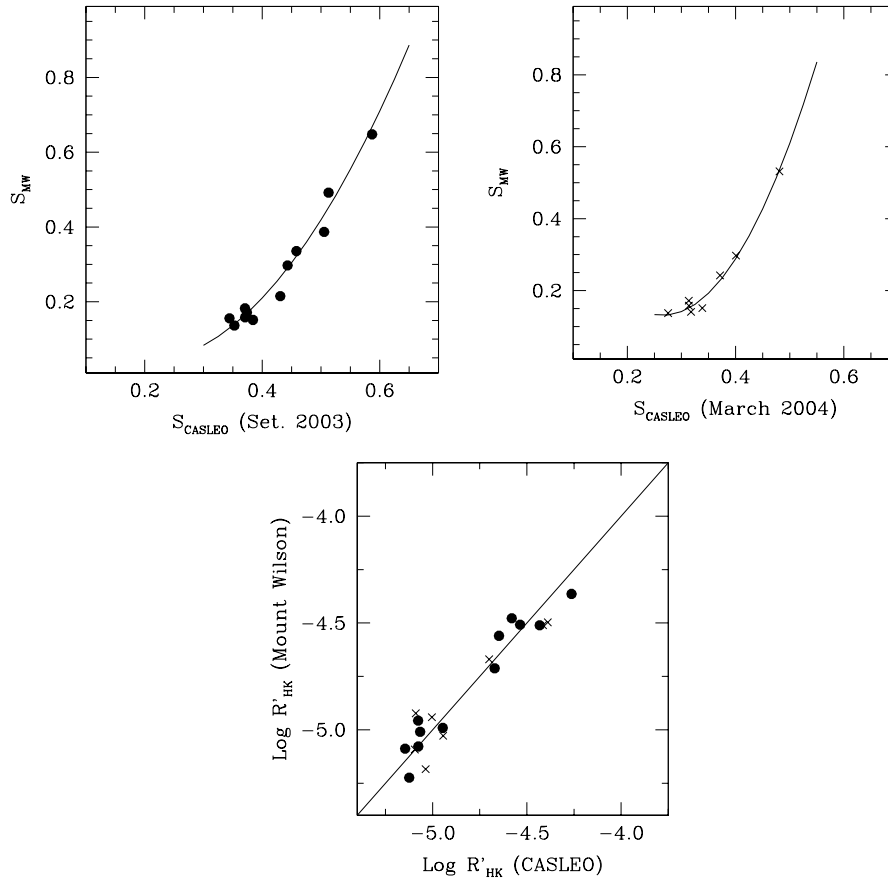


Fig. 1. Upper panel: S_{CASLEO} vs S_{MW} (MW: Mount Wilson) for the "standard" stars in Table 1 corresponding to the September 2003 and March 2004 observing runs. Lower panel: $\text{Log } R'_{HK}$ values for both observing sites (i.e., CASLEO and Mount Wilson). The open circles indicate 2003 data and the crosses 2004 observations.

and 6 of Table 3 for the stars observed at the CASLEO and in columns 3 and 4 of Table 4 for the objects with chromospheric activity index, $\text{Log } R'_{HK}$, compiled from the literature.

These calibrations are strictly valid for chromospherically quiet (i.e., $\text{Log } R'_{HK} < -4.75$; Vaughan & Preston 1980) late-type F and G dwarfs. Moreover, Wright (2004) showed that the canonical chromospheric activity-age relation breaks down for the less active stars (i.e., with $\text{Log } R'_{HK} < -5.1$). In our case, 66% of the sample (74 out of 112 stars) in Tables 3 and 4 has $-5.1 < \text{Log } R'_{HK} < -4.75$, whereas 38 objects (i.e., 34% of the sample) have $\text{Log } R'_{HK}$ values outside this range. The latter objects may have less reliable chromospheric age determinations.

Adopting the D93 calibration the range of ages corresponding to the above $\text{Log } R'_{HK}$ limits, goes from ~ 2.2 to 5.6 Gyr. However, the D93 calibration has been used beyond the Wright (2004)'s limit of $\text{Log } R'_{HK} = -5.1$ (see, for example, Henry et al. 1997; Marcy et al. 1999; Donahue 1998; Henry et al. 2000a; Pepe et al. 2004; Wright et al. 2004).

Pace & Pasquini (2004) used high-resolution spectra to derive the chromospheric activity-age relationship for a set of 5 clusters, spanning a range of age from 0.6 to 4.5 Gyr. Specifically the group of clusters analyzed by these authors includes

two young objects (Hyades and Praesepe with ages of ~ 0.6 Gyr), two intermediate age clusters (IC 4651 and NGC 3680 with ages of ~ 1.7 Gyr) and M 67, a relatively old object (age of ~ 4.5 Gyr). They obtained spectroscopic data for 21 stars which belong to the young clusters, 7 stars in the intermediate age objects and 7 stars in M 67. They found that the two intermediate age clusters show similar Ca II K activity level to the older M 67 and the Sun itself. The chromospheric activity-age relationship seems to decrease very rapidly between 0.6 and about 2 Gyr, after which it enters in a plateau.

This result imposes a serious limitation on the applicability of the chromospheric technique to derive ages for relatively old stars, with ages > 2 Gyr. In particular in the case of the EH stars, 85% of the sample (95 out of 112) has ages older than the above limit, using D93's calibration (see Tables 3 and 4), and thus the chromospheric activity as age indicator would have little practical use.

Pace & Pasquini (2004)'s stellar sample is relatively small. In particular their result is based on 7 high resolution spectra of intermediate age stars. It would be desirable to extend this analysis to include additional objects per cluster and a relatively larger number of clusters. This would help to discard any pe-

Table 2. Chromospheric index compilation for the EH stars: A sample page

Name	S	Log R' _{HK}	Data Type	Ref
HD 10697	0.1279		1 obs in 1 day (01/09/78 to 01/09/78)	R19
	0.1423		2 obs in 10 days (15/11/79 to 24/11/79)	R19
		-5.02	35 obs in 3 years	R34
	0.149	-5.08	57 obs in 25 month bins	R52
HD 12661		-5.00	1 obs 1998–99	R33
	0.14	-5.12	30 obs in 2 years	R38
	0.150	-5.08	52 obs in 16 month bins	R52
HD 16141	0.145		1979 individual	R05
	0.145		R1; R6; R5; R10; R3	R17
	0.1452		1 obs in 1 day (15/11/79 to 15/11/79)	R19
		-5.05	46 obs in 4 years	R37
	0.145	-5.11	70 obs in 23 month bins	R52
	0.085		individual	CASLEO
HD 17051	0.225	-4.65	1992 individual	R28
		-4.65		R66
	0.2074		individual	CASLEO
HD 19994	0.173	-4.88	12 obs in 4 month bins	R52
		-4.77	45 obs in 6 years	R53
	0.1018		individual	CASLEO
HD 20367	0.282	-4.50	2 obs in 1 month bins	R52
HD 23079	0.164	-4.94	1992 individual	R28
		-4.96	individual	R41
	0.1196		individual	CASLEO
HD 23596	0.150	-5.06	1 obs in 1 month bins	R52
HD 27442	0.062		individual	CASLEO
HD 28185		-5.00	1 obs 1998–99	R33
	0.143		individual	CASLEO
HD 30177		-5.08	individual	R41
	0.1205		individual	CASLEO
HD 33636		-4.81	21 obs in 3 years	R45
	0.180	-4.85	25 obs in 13 month bins	R52
	0.135		individual	CASLEO

culiarity in IC 4651 and NGC 3680 and put Pace & Pasquini (2004)’s results on more statistically solid grounds. On the other hand, Wright (2004)’s analysis is based on roughly 3000 near-by stars, one third of which has high resolution data. For the time being and in view of Pace & Pasquini (2004)’s result we will indicate how the 2 Gyr cut-off in the chromospheric activity age relation affects our analysis for the EH stars.

The uncertainty in the ages derived by the CE method strongly depends on how well the activity cycle for a particular object has been monitored (see, for example, Donahue 1998). For example, Henry et al. (2000a) estimated that if the star happens to be in a phase similar to the Solar Maunder minimum, which can last for several decades, the CE age estimation can be overestimated by ~ 2 –5 Gyr. However, if the star is in a “maximum” phase of the activity cycle the uncertainty in the age may be smaller. Henry et al. (1996) noted that the D93 relation yields ages such as in 15 out of 22 binaries the ages differ by less than 0.5 Gyr. In general, Gustafsson (1999) has estimated a typical uncertainty in the ages derived by the CE method of roughly 30%.

The sample of EH stars has at least 19 multiple systems (Udry et al. 2004), including three close binaries, γ Cep

(Hatzes et al. 2003), HD 41004 A and B (Santos et al. 2002; Zucker et al. 2004), and GJ 86 (Queloz et al. 2000). Assuming that the binary components are coeval, Donahue (1998) found that the age discrepancy between both stars has the same order as the uncertainty in the chromospheric age derivation itself. He found that for stars older than 2 Gyr, the age uncertainty is typically below 1 Gyr. This difference is, then, probably due to non-synchronized phases in the activity cycle at which each individual star has been monitored. Tidal interactions may, in principle, affect the stellar activity in close systems. However, the analyzed sample includes a relatively small number of these type of binaries and thus this effect cannot significantly alter our statistical results.

An enhancement in the CE due to the presence of a close giant planetary companion has been investigated by several authors (see, for example, Cuntz et al. 2000; Saar & Cuntz 2001; Shkolnik et al. 2003). Moreover, Rubenstein & Schaefer (2000) suggested that close giant planets may stimulate the presence of “superflares” on the CE of the EH stars. Santos et al. (2003a) proposed that the photometric variability observed in HD 192263 may also be related to the star-planet interaction effect. Other EH stars have been

Table 2. Continued. References

CASLEO: this paper	R23: Montes et al. (1997)	R46: Tinney et al. (2002b)
R01: Vaughan & Preston (1980)	R24: Montes & Martin (1998)	R47: Marcy et al. (2002)
R02: Duncan (1981)	R25: Montes et al. (1999)	R48: King et al. (2003)
R03: Soderblom (1985)	R26: Donahue et al. (1996)	R49: Butler et al. (2003)
R04: Soderblom et al. (1993)	R27: Baliunas et al. (1996)	R50: Mayor et al. (2003)
R05: Middelkoop (1982)	R28: Henry et al. (1996)	R51: Hatzes et al. (2003)
R06: Vaughan et al. (1981)	R29: Saar & Osten (1997)	R52: Wright et al. (2004)
R07: Middelkoop et al. (1981)	R30: Marcy et al. (1998)	R53: Mayor et al. (2004)
R08: Durney et al. (1981)	R31: Marcy et al. (1999)	R54: Butler et al. (2004)
R09: Baliunas et al. (1983)	R32: Fischer et al. (1999)	R55: Fischer et al. (2005)
R10: Noyes et al. (1984)	R33: Strassmeier et al. (2000)	R56: Lovis et al. (2005)
R11: Montesinos et al. (1987)	R34: Vogt et al. (2000)	R57: Sozzetti et al. (2004)
R12: Marcy et al. (1997)	R35: Udry et al. (2000)	R58: Fischer et al. (2002b)
R13: Lachaume et al. (1999)	R36: Charbonneau et al. (2000)	R59: Butler et al. (2000)
R14: Herbig (1985)	R37: Marcy et al. (2000b)	R60: Santos et al. (2004a)
R15: Soderblom & Clements (1987)	R38: Fischer et al. (2001)	R61: Santos et al. (2000b)
R16: Houvelin et al. (1988)	R39: Naef et al. (2001)	R62: Henry et al. (2000b)
R17: Young et al. (1989)	R40: Pepe et al. (2002)	R63: Butler et al. (1998)
R18: Strassmeier et al. (1990)	R41: Tinney et al. (2002a)	R64: Jones et al. (2003)
R19: Duncan et al. (1991)	R42: Fischer et al. (2002a)	R65: Marcy et al. (2001)
R20: Soderblom et al. (1991)	R43: Butler et al. (2002)	R66: Rocha-Pinto & Maciel (1998)
R21: Soderblom & Mayor (1993)	R44: Udry et al. (2002)	
R22: Baliunas et al. (1995a)	R45: Vogt et al. (2002)	

searched for an enhancement in the CE due to the presence of a close planet (Saar & Cuntz 2001; Shkolnik et al. 2004).

Shkolnik et al. (2003) found evidence for a planet-induced chromospheric activity in the EH star HD 179949, having a planetary companion with a semi-major axis of ~ 0.04 AU (an orbital period of ~ 3 days). The planet period is synchronized with the enhancement of the CE, which increases by $\sim 4\%$ when the planet passes in front of the star. Translated into ages, this would represent a difference of 0.8 Gyr for a 5 Gyr EH star, adopting the D93 calibration. This difference is about the same as the uncertainty in the chromospheric ages. A similar effect was detected in ν And (Shkolnik et al. 2003, 2004).

We have searched for correlations between the CE (measured by $\text{Log } R'_{\text{HK}}$) and the orbital parameters of the associated planet, such as: $M \sin i$, e , and a . Figure 2 shows the $\text{Log } R'_{\text{HK}}$ vs the semi-major axis, a , plot, as an example. In this figure, 51 Peg-like stars (i.e., those with a < 0.1 AU) are indicated with filled circles whereas the rest of the sample is with empty symbols. In general, no clear trend is found between the CE and the planet orbital parameters. However, the chromospheric ages may be affected, particularly in the cases of HD 179949, HD 192263, and ν And. In any event, we expect that the CE enhancement, due to the presence of a close giant planet, to be in about the same order as the uncertainty in the chromospheric ages in view of the amount of this effect for HD 179949, as discussed above.

Recently, Wright et al. (2004) have derived the CE for a sample of ~ 1200 F-, G-, K- and M- type main-sequence stars, using archival spectra from the California & Carnegie Planet Search Project. To somehow compensate or smooth the effect of the stellar variability in an uneven sampling set of

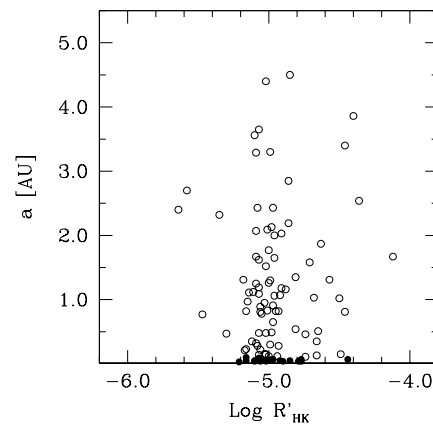


Fig. 2. CE (measured by $\text{Log } R'_{\text{HK}}$) versus the semi-major axis a , for the EH sample. 51 Peg-like objects (i.e., those with a < 0.1 AU) and the rest of the sample are represented by filled and empty circles, respectively.

data, they used the median S-values in 30-day bins and then adopted the median value of those medians (the "grand-S" value). The number of interval-bins typically vary between a few and few tenths, during a period of time of more than ~ 6 years. These authors derived ages by applying the D93 calibration. As Wright et al. (2004)'s sample includes 63 EH stars, in Figure 3 we compare their values of $\text{Log } R'_{\text{HK}}$ and ages with the ones reported in this paper, excluding, in this case, Wright et al. (2004)'s data from our compilation (see Table 2).

We notice a general agreement between the CE indexes (and the corresponding ages) derived by Wright et al. (2004)

Table 3. Chromospheric index, $\text{Log } R'_{\text{HK}}$, and age for the EH stars observed at the CASLEO

Name	$\text{Log } R'_{\text{HK}}_{\text{CASLEO}}$	$\langle \text{Log } R'_{\text{HK}}_{\text{without CASLEO}} \rangle$	$\langle \text{Log } R'_{\text{HK}}_{\text{with CASLEO}} \rangle$	D93 Age[Gy]	RPM98 Age[Gy]
GJ 86	-4.67	-4.74	-4.72	2.03	2.94
HD 142	-5.11	-4.92	-5.02	5.93	2.43
HD 1237	-4.31	-4.36	-4.34	0.15	0.25
HD 2039	-5.06	-4.91	-4.98	5.28	1.20
HD 4208	-4.94	-4.94	-4.94	4.47	6.03
HD 6434	-5.23	-4.89	-5.06	6.85	18.51
HD 17051	-4.58	-4.65	-4.63	1.47	0.43
HD 19994	-5.76	-4.83	-5.14	8.91	2.56
HD 23079	-5.23	-4.95	-5.04	6.53	5.92
HD 27442	-5.57		-5.57	24.74	7.15
HD 28185	-4.98	-5.00	-4.99	5.36	1.69
HD 30177	-5.15	-5.08	-5.12	8.30	1.50
HD 33636	-5.03	-4.83	-4.90	3.83	3.24
HD 38529	-5.07	-4.93	-4.97	5.09	0.89
HD 39091	-4.82	-4.97	-4.90	3.83	1.83
HD 52265	-4.90	-4.97	-4.96	4.88	1.65
HD 72659	-4.79	-5.01	-4.94	4.42	2.62
HD 73526	-5.00		-5.00	5.59	1.49
HD 75289	-4.94	-4.98	-4.97	4.96	1.29
HD 76700	-4.94		-4.94	4.51	0.77
HD 82943	-4.77	-4.87	-4.84	3.08	0.72
HD 83443	-4.79	-4.85	-4.83	2.94	0.63
HD 92788	-4.95	-4.88	-4.89	3.78	0.87
HD 108147	-4.64	-4.75	-4.71	1.98	0.70
HD 114386	-4.74		-4.74	2.19	1.91
HD 114729	-4.67	-5.04	-4.95	4.58	6.35
HD 114783	-4.70	-4.98	-4.89	3.70	1.82
HD 121504	-4.67	-4.65	-4.66	1.62	0.66
HD 130322	-4.63	-4.56	-4.58	1.24	0.77
HD 134987	-5.13	-5.05	-5.08	7.32	1.77
HD 141937	-4.77	-4.80	-4.79	2.55	1.25
HD 142415	-4.69	-4.61	-4.63	1.49	0.51
HD 147513	-4.40	-4.46	-4.45	0.65	0.45
HD 160691	-5.10	-5.02	-5.04	6.41	1.45
HD 162020	-4.12		-4.12	0.00	0.23
HD 168443	-5.00	-5.02	-5.02	5.90	3.13
HD 168746	-4.92	-4.87	-4.89	3.75	3.18
HD 169830	-5.05	-4.94	-4.97	4.95	1.62
HD 179949	-4.66	-4.76	-4.72	2.05	0.68
HD 202206	-4.72		-4.72	2.04	0.44
HD 210277	-5.02	-5.07	-5.06	6.93	2.25
HD 213240	-5.12	-4.90	-4.97	5.11	1.90
HD 216435	-4.95	-5.00	-4.98	5.27	1.56
HD 216437	-5.52	-5.01	-5.27	12.96	3.98
HD 217107	-5.17	-5.05	-5.08	7.32	1.40
HD 222582	-5.05	-5.00	-5.03	6.16	3.38

and our compilation. The median difference in $\text{Log } R'_{\text{HK}}$ is 0.04 dex (with a standard deviation of 0.05 dex), implying a median age discrepancy of ~ 0.4 Gyr (0.8 Gyr for the standard deviation) for a 5 Gyr star. The largest CE (and age) differences correspond to the stars HD 19994, HD 89744 and HD 130322, see Table 5. These objects are marked in Figure 3 with the letters A, B and C, respectively.

4. Derivation of ages for the EH stars applying other methods

In this section we apply four other techniques to infer ages for the EH group and compare these results with the chromospheric determinations.

Table 4. Chromospheric index, Log R'_{HK} , and age for the EH stars not observed at the CASLEO

Name	$\langle \text{Log } R'_{\text{HK}} \rangle$	D93 Age[Gy]	RPM98 Age[Gy]	Name	$\langle \text{Log } R'_{\text{HK}} \rangle$	D93 Age[Gy]	RPM98 Age[Gy]
16 Cyg B	-5.09	7.59	3.79	HD 80606	-5.09	7.63	1.73
47 Uma	-5.02	6.03	3.2	HD 88133	-5.16	9.56	6.27
51 Peg	-5.05	6.6	2.21	HD 89744	-5.11	8.09	2.55
55 Cnc	-5.00	5.5	1.21	HD 93083	-5.02	6	3.86
70 Vir	-5.07	7.09	5.52	HD 99492	-4.94	4.49	2.93
BD-103166	-4.92	4.18	0.53	HD 101930	-4.99	5.39	3.48
ϵ Eri	-4.46	0.66	0.82	HD 102117	-5.03	6.21	2.99
γ Cephei	-5.32	14.78	6.39	HD 104985	-5.58	25.35	27.08
GJ 436	-5.21	11.05	7.41	HD 106252	-4.97	5.02	3.36
GJ 876	-5.17	9.9	6.52	HD 108874	-5.08	7.26	2.21
GJ 777A	-5.07	7.09	2.08	HD 111232	-4.98	5.2	9.65
HD 3651	-4.98	5.13	2.25	HD 117618	-4.90	3.88	2.72
HD 4203	-5.16	9.41	1.66	HD 128311	-4.40	0.39	0.41
HD 8574	-5.07	7.13	3.79	HD 136118	-4.93	4.26	3.16
HD 8673	-4.71	1.95	0.01	HD 145675	-5.09	7.6	1.20
HD 10697	-5.12	8.48	3.49	HD 150706	-4.57	1.17	0.83
HD 11964	-5.16	9.56	6.27	HD 154857	-5.14	8.98	14.29
HD 12661	-5.07	7.05	1.39	HD 177830	-5.35	15.89	4.03
HD 16141	-5.09	7.76	3.08	HD 178911 B	-4.98	5.2	1.54
HD 20367	-4.50	0.87	0.37	HD 187123	-4.99	5.33	2.26
HD 23596	-5.06	6.89	1.61	HD 190228	-5.18	10.16	14.29
HD 37124	-4.86	3.33	6.68	HD 192263	-4.44	0.57	0.55
HD 40979	-4.63	1.48	0.51	HD 195019	-4.99	5.33	2.58
HD 41004A	-4.66	1.64	1.48	HD 196050	-4.85	3.17	1.03
HD 45350	-5.00	5.59	1.94	HD 208487	-4.90	3.88	4.06
HD 46375	-4.97	4.96	1.68	HD 209458	-4.95	4.72	2.88
HD 49674	-4.77	2.38	0.55	HD 216770	-4.88	3.6	1.02
HD 50554	-4.95	4.58	2.89	HD 219449	-5.47	20.76	18.24
HD 50499	-5.02	6	1.82	HD 330075	-5.03	6.21	3.09
HD 68988	-5.06	6.78	1.34	ρ Crb	-5.06	6.94	8.48
HD 70642	-4.90	3.88	1.42	τ Boo	-4.78	2.52	0.80
HD 73256	-4.49	0.83	0.26	TrES-1	-4.77	2.41	1.63
HD 74156	-5.08	7.38	2.83	ν And	-4.99	5.32	2.26

Table 5. EH stars with the largest CE and age differences

Name	Log R'_{HK} this paper	Log R'_{HK} Wright et al. (2004)	Age [Gyr] this paper	Age [Gyr] Wright et al. (2004)	Label in Figure 3
HD 19994	-5.27	-4.88	13.01	3.55	A
HD 89744	-5.12	-4.94	8.29	4.47	B
HD 130322	-4.51	-4.78	0.93	2.45	C

4.1. Isochrones

The T_{eff} and the luminosity of a star allow us to place it on the theoretical HR diagram. This position changes as the star evolves. The age of a given star can, at least in principle, be inferred adopting an evolutionary model and the corresponding isochrones. However, in practice, the derivation of reliable isochrone ages is a difficult task.

Isochrone ages are usually calculated by comparing the position of the star on the HR diagram with the set of isochrones adopted. This procedure is particularly complicated for low mass objects for which isochrones are curved and approximate one to the other. Apart from this, the uncertainties in the ob-

servables (i.e., T_{eff} , luminosity and metallicity) can seriously limited the applicability of this technique. Pont & Eyer (2004) have extensively discussed the influence on the age derivation of these uncertainties. In addition these authors have developed a method based on Bayesian probability to treat systematic bias and large uncertainties in the observables to derive more reliable ages. In particular the use of this method allowed a considerable reduction the intrinsic dispersion in the $[\text{Fe}/\text{H}]$ -age relation (see Pont & Eyer 2004).

Recently Nördstrom et al. (2004) have determined ages for about 13636 nearby stars, including the EH group, using the Padova isochrones (Girardi et al. 2000; Salasnich et al. 2000). This set of isochrones covers the range of ages be-

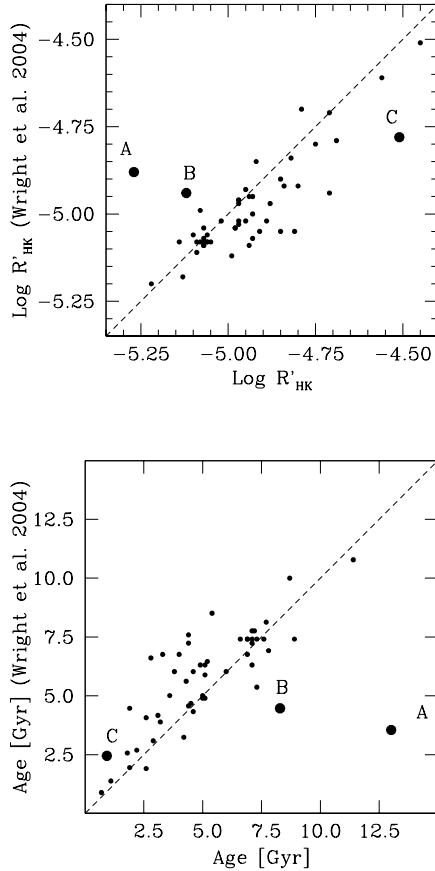


Fig. 3. Comparison between the CE index, $\text{Log } R'_{\text{HK}}$, and the age for the H sample stars derived by Wright et al. (2004) and those reported in this contribution. To make these comparisons we have used stars in common and eliminated Wright et al. (2004)’s data from the averages reported in Table 2. The ages have been obtained from the D93 calibration. The large circles indicate stars with the largest discrepancies: (A) HD 19994, (B) HD 89744 and (C) HD 130322, see Table 5.

tween 0 and 17.8 Gyr. Nördstrom et al. (2004) give the age for a given star if it lies within 1σ upper and lower limits of the nearest isochrone trace. Otherwise, only upper or lower limits are determined. In Table 7, columns 2, 3 and 4, we list the ages and/or lower and upper limits derived by these authors for the EH group. As mentioned before, our purpose is to compare the ages derived by applying different methods. The compilation of ages from Nördstrom et al. (2004) in Table 7 is useful to this purpose.

Nördstrom et al. (2004) have provided estimations of errors in their age determinations. As mentioned above their sample includes 13636 stars, with 84% of the objects lying within 1σ upper and lower limits. In addition, 82% of these stars has estimated relative errors below 50%, and 47% of these even below 25%. We follow Nördstrom et al. (2004) to quote errors for the isochrone ages for the EH stars. 77% (61 out of 79) of the EH sample lies within 1σ upper and lower limits. 44% of

these objects (27 out of 61) has estimated relative errors below 50% and 10% of these (6 out of 61) even below 25%. On average, we assume a ”typical” error of $\sim 50\%$ in the isochrone age determinations.

We note that Nördstrom et al. (2004) carried out a careful and detailed error estimation for the isochrone technique (the reader is referred to their work for the description of the method applied). In general, these authors derived larger uncertainties than those classical ones obtained (see, for example, Gustafsson 1999; Edvardsson et al. 1993). However, Nördstrom et al. (2004)’s error analysis seems more realistic than those performed before. In addition, these authors have also compared their age derivations with those computed using the Bayesian method of Pont & Eyer (2004), finding no significant differences due to the procedures themselves.

4.2. Lithium abundance

The lithium content in the stellar atmosphere is destroyed as the convective motions gradually mix the stellar envelope with the hotter ($T \sim 2.5 \times 10^6$ K) inner regions. Thus a lithium-age relation may be expected. However, this relation is poorly constraint. For instance, while Boesgaard (1991) derived a lithium-age relation for stars with $5950 \text{ K} < T_{\text{eff}} < 6350 \text{ K}$ belonging to eight open clusters, Pasquini et al. (1994) and Pasquini et al. (1997) found a factor of 10 for the lithium abundance for stars at given T_{eff} in M67, an open cluster with almost the solar age and metallicity.

The lithium abundance of EH and field stars has been compared in the literature. Gonzalez & Laws (2000) suggested that the EH stars have less lithium than field stars, while Ryan (2000) proposed that both groups have similar lithium abundance. Recently, Israelian et al. (2004) found a likely excess of lithium depletion in EH stars with T_{eff} in the range 5600–5850 K, in comparison to field stars in the same range of temperatures. For an average difference of ~ 1.0 dex in the lithium content of the two groups, the EH stars are ~ 2 Gyr older than field stars, according to the lithium-age relation derived by Soderblom (1983). On the other hand, Israelian et al. (2004) did not find a significant difference for EH and field stars with T_{eff} in the range 5850–6350 K.

We apply this method only as an additional age indicator to compare with the other techniques. We obtained lithium abundances, $\text{Log } N(\text{Li})$, for the sample EH stars from Israelian et al. (2004) and used the calibration of Soderblom (1983) to derive ages for these objects. This relation is valid for solar-type stars with abundances intermediate to the Hyades and the Sun (i.e., $0.95 < \text{Log } N(\text{Li}) < 2.47$). 20 EH stars are included within these limits. This range in the Li abundances introduces a bias toward younger ages and prevents us from making a meaningful comparison with the other estimators. We then use the Soderblom (1983) calibration to derive individual stellar ages for the EH stars when having Li abundances within the valid range. In Table 7 column 5 gives the obtained ages. For HD 12661 only an upper limit to the lithium abundance was avail-

able and thus we derived a lower limit to the age of this object. The subindex "L" in Table 7 indicates so.

Boesgaard (1991) derived a lithium-age calibration valid over a larger range in Li abundances, $2.1 < \text{Log } N(\text{Li}) < 3.0$, but restricted to stars with $5950 \text{ K} < T_{\text{eff}} < 6350 \text{ K}$. This temperature range comprises $\sim 20\%$ of the EH sample. In addition, considering both the Li abundances and the T_{eff} intervals, the Boesgaard (1991)'s calibration can be applied to obtain ages for only 9 EH stars. For this reason we chose the Soderblom (1983)'s calibration over the Boesgaard (1991)'s relation. We note that these calibrations are complementary in metallicity range, however they do not provide a reasonably good agreement within the metallicity interval held in common, thus preventing the application of both calibrations together in our age estimations.

4.3. Metallicity

The production of heavy elements in the stellar cores during the life time of the Galaxy enriches the interstellar medium from which new stars are formed. Thus an age-metallicity relation may be expected. Twarog (1980) and Edvardsson et al. (1993) studied the disk population and found a relatively weak correlation between these two quantities. The scattering in metallicity for a given age is so large that some authors have even questioned the existence of a correlation between these two parameters (see, for example, Feltzing et al. 2001; Ibukiyama & Arimoto 2002; N rdstrom et al. 2004). Other works have been aimed to improve this relation, trying to disentangle the different possible contributions to the dispersion (e.g., Ng & Bertelli 1998; Reddy et al. 2003). In particular, Pont & Eyer (2004) have shown that at least part of the scattering in the original Edvardsson et al. (1993)'s age-metallicity relation is mainly due to systematic bias affecting the ages derived by the isochrones method. However, in spite of these efforts, the dispersion at each given age is still rather large. Nevertheless, the use of the age-metallicity relation as an independent age estimator can provide some constraints to the EH stars age distribution and a manner to check the results derived by the chomospheric method.

We obtained the spectroscopic [Fe/H] data for the sample of EH stars from Santos et al. (2004b) whenever possible, otherwise we used the data from N rdstrom et al. (2004). We adopted the age-metallicity relation of Carraro et al. (1998) and followed the procedure outlined by Lachaume et al. (1999) only to derive upper limits to the ages of the EH stars, due to the large scattering in this relation.

We defined an upper envelope to the data points in the Carraro et al. (1998) relation, binning these data in 3 Gyr intervals and calculating the average [Fe/H] and the corresponding dispersion. We adopted as the upper limit the average [Fe/H] plus the rms values in each bin. We then fitted these points with a quadratic polynomial by least squares, giving t_{max} (an upper limit to the age) as function of the metallicity. Table 6 lists the data derived from Carraro et al. (1998) used to calculate the following relation:

Table 6. Data points used to calculate Equation 5 derived from Carraro et al. (1998)

[Fe/H]	t_{max} [Gyr]
0.15	1.5
0.07	4.5
-0.02	7.5
-0.14	10.5
-0.35	13.5

$$t_{\text{max}} = -35.847 [\text{Fe}/\text{H}]^2 - 31.172 [\text{Fe}/\text{H}] + 6.9572. \quad (5)$$

Equation 5 is valid for $-0.35 < [\text{Fe}/\text{H}] < 0.15$ or $1.5 < t_{\text{max}} < 13.5$ Gyr. This range of metallicities is appropriate for 44% (50 out of 114) of the EH objects, for which it was possible to apply this age estimator. This range excludes the most metal-rich EH stars, introducing a bias toward older ages. Table 7 in column 6 lists metallicity derived ages for the individual objects comprised within the before mentioned range of metallicity. Carraro et al. (1998) data can also be used to derive a lower metallicity-age limit. The resulting relation includes only 11% (13 out of 114) of the EH objects, due to their metal-rich nature.

4.4. Kinematics

The velocity dispersions of a coeval group of stars increases with time (Parenago 1950; Roman 1954; Dehnen & Binney 1998; Binney et al. 2000). The kinematics of a given group can be used as an age estimator for the group rather than to derive individual stellar ages. In particular, the transverse velocity dispersion S (i.e., the dispersion of the velocity components perpendicular to the line of sight) of a sample of stars may be used with this purpose (Binney et al. 2000).

We derived S for a sample of solar neighborhood stars, to compare with the EH group. The first sample was constructed in the same manner described by Dehnen & Binney (1998). These authors selected a kinematically unbiased solar neighborhood group isolating a magnitude-limited subsample, composed by single main sequence stars with relative parallax errors smaller than 10% obtained from the Hipparcos catalog. In what follows we briefly outline Dehnen & Binney (1998)'s procedure to define such a sample.

Due to the lack of completeness in the Hipparcos catalog⁴, Dehnen & Binney (1998) used the Tycho catalog to construct a combine sample that they estimated to be 95% complete. The Hipparcos catalog was divided in $16 \times 16 \times 10$ uniformly spaced bins in $\sin b$, Galactic longitude l and $B-V$. All stars brighter in magnitude than the second brightest star per bin included in Tycho and not in the Hipparcos catalog were added to this bin. In our case this gave a list of 8864 stars.

A second sample was constructed from the Hipparcos Proposal 018, containing 6845 stars within 80 pc and south of -28 deg, which have been spectrally classified by the Michigan Catalog by 1982 (Houk & Cowley 1975; Houk 1978, 1982). Of these stars, 3197 are main-sequence single objects with rel-

⁴ See Dehnen & Binney (1998) for details on this issue.

ative parallax errors smaller than 10%. The union of these two groups provides a kinematically unbiased sample of 12061 stars (see also Dehnen & Binney 1998).

The velocity dispersion S for each star was derived following the formalism of Dehnen & Binney (1998). Figure 4 shows the S vs $B-V$ diagram for the solar neighborhood with open squares. $B-V$ colors were also obtained from the Hipparcos catalog and dereddened according to the spectral types, given in the same catalog. We used a sliding window of 500 objects and plotted a point every time a 100 stars are left out from the window. We have tested different sizes for the sliding window and found no significant differences. The global change in the slope at $B-V \sim 0.6$ for solar neighborhood stars in Figure 4 is called Parenago’s discontinuity, and it has recently been quantified by Dehnen & Binney (1998). At the red side of this point, stars of every age are found, while at the blue side the most recently formed objects lie. The discontinuity itself corresponds to the $B-V$ color at which the main sequence lifetime of a star equals the age of the Galactic disk (Dehnen & Binney 1998). The general trend of the solar neighborhood sample in Figures 4 is very similar to that derived by Binney et al. (2000).

We obtained S for the EH sample including stars with relative parallax error less than 10%. This excludes 7 out of 131 EH stars with parallax data (i.e., 5% of the group). However we were unable to apply the single and main sequence stars criteria as these would eliminate $\sim 42\%$ of the objects. In Figure 4, with filled circles, we superimpose the results for the EH stars to compare with the solar neighborhood sample. For the EH group we chose a sliding window of 30 objects and plotted a point when 6 stars have left the window. On the right side of Figure 4 we indicate the age scale derived by Binney et al. (2000).

EH stars seem to have similar transverse velocity dispersions to the solar neighborhood stars, with an average age of about 4–6 Gyr. However, most EH stars lie to the right of Parenago’s discontinuity, where the kinematic method becomes less reliable.

Manoj & Bhatt (2005) analyzed the sample of Vega-like candidate stars, (main sequence) stars that show infrared excesses, attributed to the presence of circumstellar dust ($T \sim 50$ – 125 K), warmed by the central object (e.g., Zuckerman 2001). They found that the transverse velocity dispersions are systematically smaller than for solar neighborhood stars, suggesting a younger age for the Vega-like sample with respect to the solar neighborhood. As most of the Vega-like stars have A spectral type, the sample lies to the left of Parenago’s discontinuity, where the kinematic method can safely be applied.

As an additional test we have used the space velocity components (U , V , W) to check the consistency of the results. Reid (2002) has recently applied this technique to derive a lower limit to the age of a group of 67 EH stars. We extend this analysis to include 101 of the presently known EH stars with space velocity data available. We followed the kinematic method described by Lachaume et al. (1999), using values of U , V and W for the EH stars from Nördstrom et al. (2004) and correcting them by the Solar Motion (-13.4 , -11.1 , $+6.9$ Km/s;

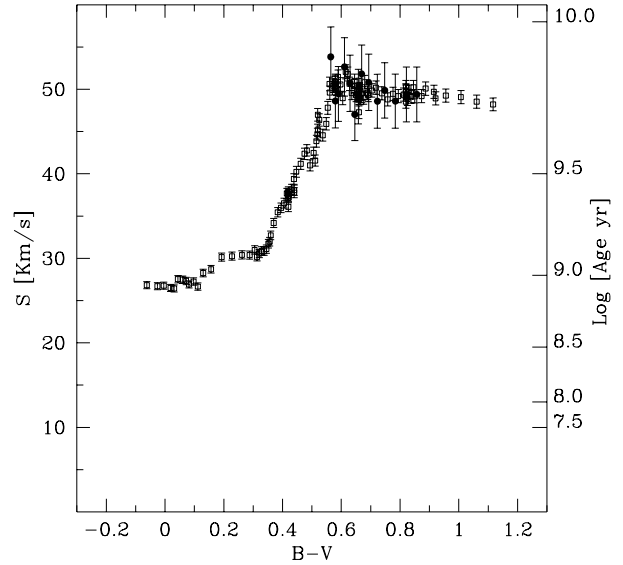


Fig. 4. Transverse velocity dispersion S vs dereddened $B-V$. Solar neighborhood stars and EH stars are represented by squares and filled circles, respectively. Error bars are derived as $\Delta S = S / \sqrt{2n - 2}$, where n is the number of objects per bin. The age scale on the right side was obtained from Binney et al. (2000).

Chen et al. 1997). We derived a lower limit of 3.9 ± 2.9 Gyr for the sample of EH stars, which agrees with the average age derived using the transverse velocity dispersions (i.e., 4–6 Gyr). We caution, however, that the later kinematic method is less reliable as an age estimator because EH stars lie red-ward of Parenago’s discontinuity.

The kinematic properties of the EH stars have also been investigated by other authors. As mentioned before, Reid (2002) used the space velocity components to infer a lower limit to the age for the EH sample. Other groups have confronted kinematic and metallicity properties of the EH stars with those of similar stars with non known planets. The aim of these works was to analyze whether the kinematics of the EH stars may provide a hint to explain the relatively high metallicities of the EH stars.

For example, Gonzalez (1999) analyzed the chemical and dynamical properties of the EH stars within the framework of the diffusion of stellar orbits in space (Wielen et al. 1996). With this purpose he confronted the EH group which is metal rich with a sample of F and G dwarfs and subgiants with well determined metallicities, ages and kinematics. He concluded that the stellar diffusion model is not able to account for the high metallicity in EH stars.

Barbieri & Gratton (2003) compared the galactic orbits of EH stars with those of stars with no known planets taken from the catalog of Edvardsson et al. (1993). Both groups are not kinematically different. However at each perigalactic distance the EH stars have systematic larger metallicities than the average of the comparison sample. This result was recently con-

Table 8. Medians and standard deviations for EH star age distributions

Method	Age [Gyr]	σ [Gyr]	No. of stars
Chromospheric RPM98	1.9	4.0	112
Chromospheric D93	5.2	4.2	112
Isochrone lower limit	4.8	3.0	75
Isochrone	7.4	4.2	79
Isochrone upper limit	9.2	3.9	69

firmly by Laws et al. (2003). The latter authors also found evidence of a difference in the slope of the metallicity- Galactocentric radius relation between star with and without planets. Due to the metal rich nature of the EH stars, these objects have a steeper slope than the comparison group.

Santos et al. (2003b) analyzed the space velocities of EH stars and stars with no planet/s detected, in relation to their different metallicity abundances. They concluded that the space velocity distribution for the first objects is basically the same as for the second type of stars. However the EH stars lie on the metal-rich envelope of the no-known-planet-star population.

4.5. Comparison of ages for the EH stars derived by different methods

In this section we compare the age distributions of the EH stars derived by the chromospheric, isochrone, Li and [Fe/H] abundances. The kinematic ages are not considered here as non individual stellar ages can be obtained.

Figure 5, upper panels, shows the histogram distributions for the ages derived using the chromospheric method applying D93 and RPM98 calibrations, respectively. In this section we analyze chromospheric ages listed in Tables 3 and 4, i.e., including objects with ages exceeding the 2 or 5.6 Gyr limits suggested by Pace & Pasquini (2004) and Wright (2004), respectively (see section 3.). In the isochrone age distribution (lower panel), we include upper and lower limits with continuous and dotted lines, respectively, as derived by Nördstrom et al. (2004). Li and [Fe/H] ages are not included in the histograms of Figure 5, as the methods used (see sections 4.2 and 4.3) introduce bias toward younger and older ages, respectively. Moreover the number of EH stars with Li age is relatively small (20 objects).

The ages distribution derived from the D93 calibration is broad. On the contrary, the chromospheric age histogram obtained applying the RPM98 calibration is quite narrow, with most of the objects having ages < 4 Gyr. The isochrone age distribution is also quite broad with two maxima at 3 and 9 Gyr, respectively, probably showing the separation between F and G spectral types within the EH sample. Karatas et al. (2005) also noted that their distribution of ages for the EH stars, derived using the isochrone technique, was flat or uniform (having roughly the same number of stars in each age bin) over $3 \lesssim \text{age} \lesssim 13$ Gyr. Table 8 lists the medians and the dispersions of the histograms in Figure 5.

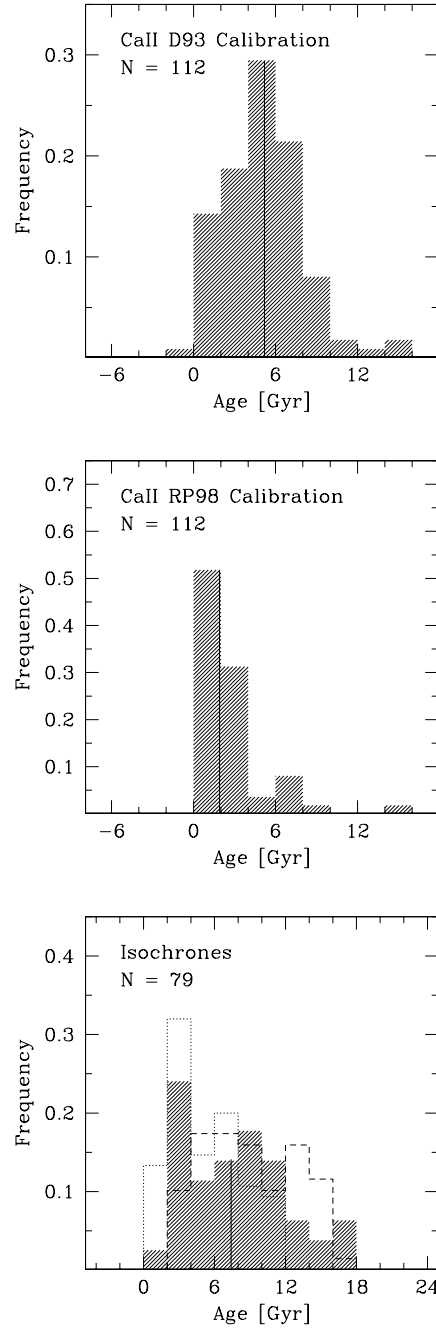


Fig. 5. Upper panels: Chromospheric age distributions derived from the D93 and RPM98 calibrations. The lower panel correspond to the isochrone distribution. Vertical continuous lines show the medians of each histogram. In the isochrone age distribution we superpose with continuous and dotted lines upper and lower limits estimations from Nördstrom et al. (2004).

The chromospheric age distributions resulting from the application of the D93 and the RPM98 calibrations are very different, with significantly different medians (see Table 8). As mentioned before the RPM98 calibration includes a metallicity correction factor whereas the D93 relation is independent

Table 7. Ages derived from isochrone, lithium and [Fe/H] abundances. “L” indicates a lower limit.

Object	Isochr. Age [Gyr]	Isochr. Min. Age [Gyr]	Isochr. Max. Age [Gyr]	Lithium Age [Gyr]	[Fe/H] Max. Age [Gyr]
16 Cyg B	9.9	5.6	13.2		4.2
47 Uma	8.7	5.3	11.9	2.0	5.0
51 Peg	9.2	4.8	12.0	3.5	
70 Vir	7.4	6.7	7.9	1.9	8.7
ϵ Eri					10.4
GJ 86					12.5
Hip 75458					2.3
ρ Crb	12.1	10.1	13.9	3.3	11.9
τ Boo	2.4	1.3	3.1		
ν And	3.3	2.8	5.0		2.3
HD 142	3.6	2.8	4.3		1.9
HD 1237		8.8			2.7
HD 2039	1.8		3.4		
HD 3651	17.0	2.6			2.7
HD 4208					12.4
HD 6434	13.3	7.0			
HD 8574	8.2	5.7	9.6		5.0
HD 8673	2.8	2.1	3.3		8.7
HD 10647	4.8		7.0		7.9
HD 10697	7.1	6.4	7.9	1.5	1.9
HD 12661				4.4	
HD 16141	11.2	9.7	12.9	4.0	
HD 17051	3.6	1.1	6.7		
HD 19994	4.7	3.1	5.2	1.4	
HD 20367	6.4	3.6	8.9		
HD 23079	8.4	5.3	12.6		10.0
HD 23596	5.4	3.1	6.7		
HD 28185	12.2	7.1		2.8	
HD 33636	8.1	0.1	13.4		9.2
HD 34445	9.5	8	11.1		7.3
HD 39091	6.0	2.9	9.0		3.5
HD 40979	6.2	3.8	9.2		
HD 41004A					9.5
HD 45350	12.6	10.4	14.6		
HD 46375	16.4	7.7			
HD 50554	7.0	3.3	9.9		6.6
HD 50499	4.3	2.8	7.4		
HD 52265	3.8	1.6	5.2		
HD 65216					10.2
HD 68988	3.7	1.5	6.1		
HD 70642	10.2	4.2	16.0		
HD 72659	8.2	6.5	9.6		6.0
HD 73256	15.9	6.4			
HD 73526	10.3	8.3	12.6		
HD 74156	3.2	2.7	3.7		
HD 75289	4.0	2.2	5.8		
HD 76700	11.5	10.0	13.1		
HD 80606			17.6		
HD 82943	3.5		7.2		

of the stellar metallicity effect. For instance, for a EH star with [Fe/H]=0.16, corresponding to the median of the EH sample (Santos et al. 2004b), the RPM98 calibration gives an age \sim 3 Gyr lower (younger) than the D93 relation. However, from

Figure 5 and Table 8 it is clear that, the age distribution derived using the D93 calibration agrees better with the isochrone ages than the distribution obtained from the RPM98 relation.

Table 7. Continued.

Object	Isochr. Age [Gyr]	Isochr. Min. Age [Gyr]	Isochr. Max. Age [Gyr]	Lithium Age [Gyr]	[Fe/H] Max. Age [Gyr]
HD 89307	8.8	3.9	13		12.2
HD 89744	2.2	2.0	2.4	1.2	
HD 92788	9.6	4.8	14.3	3.4	
HD 102117	12.6	10.9	14.3		3.9
HD 104985	3.1	2.3	3.6		
HD 106252	9.2	5.2	13.5	2.5	7.3
HD 108147	4.4	2.3	6.6		
HD 108874	14.1	10.7			
HD 111232		8.9			
HD 114386					9.2
HD 114729	11.9	10.4	13.3	1.6	12.5
HD 114762	11.8	7.9	15.1		
HD 114783					3.9
HD 117207	16.1	11.1			4.6
HD 117618	6.7	3.6	9.6		7.6
HD 121504	7.1	3.9	10.2		
HD 128311					6.0
HD 130322					6.0
HD 134987	11.1	6.4	12.6		
HD 136118	4.8	2.9	5.5		8.1
HD 141937	1.8		7.5		3.5
HD 142022	17.2	9.4			
HD 142415	2.4		7.9		
HD 147513	8.5		14.5	1.3	5.0
HD 150706	8.0		15.0		7.3
HD 154857	3.5	2.9	4.4		13.1
HD 162020					9.5
HD 168443	10.6	9.5	11.8		5.0
HD 168746	16.0	10.8			9.2
HD 169830	2.3	1.9	2.7	3.9	
HD 179949	3.3	0.4	5.4		
HD 183263	3.3	1.1	5.8		
HD 187123	7.3	3.8	10.6	3.8	2.3
HD 188015	10.8	6			
HD 190228	5.1	4.1	6.6	3.7	12.5
HD 192263					7.6
HD 195019	10.6	9.4	11.8	3.0	3.9
HD 196050	3.5	1.8	5.3		
HD 196885	8.4	7.2	9.7		
HD 202206				4.2	
HD 208487	6.6	3.8	9.3		10.8
HD 209458	6.6	3.5	9.2		6.3
HD 213240	3.6	3.0	4.2		
HD 216435	5.4	4.9	6.0		
HD 216437	8.7	7.5	9.7	1.6	
HD 216770	16.9	7.4			
HD 217107		6.5			
HD 222582	11.1	6.9	15.3		5.3
HD 330075					4.2

Feltzing et al. (2001) have suggested that the RPM98 metallicity correction is not properly defined. The correction factor for older ages is larger than for younger ages, as is given in $\Delta\text{Log age}$. We adopt the D93 calibration in spite of the rel-

atively high metal abundance of EH stars, in view of the poor determination of this effect.

In Figure 6 we plot the chromospheric ages vs the isochrone and lithium ages. In addition we show the chromospheric ages against the [Fe/H] upper limits. Chromospheric ages are sys-

tematically smaller than isochrone determinations and larger than lithium ages. However, the relatively younger lithium ages are probably only reflecting the bias introduced by the calibration used as discussed in section 4.2. The metallicity derived ages are, on average, systematically older than the chromospheric determinations (see Figure 6). As for the Li ages, this is probably due to a selection effect against metal-rich stars and thus younger objects, in this case introduced by the metallicity-age relation (see section 4.3.). We estimate a dispersion of about ~ 4 Gyr for the chromospheric, isochrone, metallicity (upper limit) ages. The lithium age distribution in Figure 6 (upper right panel) has the smallest dispersion (~ 2 Gyr), however again this is probably due to the fact that only the younger ages are taken in account. In conclusion, for the Li ages, neither the the age difference (with respect to the chromospheric ages) nor the relatively smaller dispersion are attributed to real features but rather to the lack of older stars with Li ages estimations. In the case of the [Fe/H] upper limits, the exclusion of younger objects restrain a comparison with the chromospheric ages.

The chromospheric activity is a reliable age indicator for F and G dwarfs from young ages to about ~ 2.0 Gyr, adopting the most conservative limit suggested by Pace & Pasquini (2004), or possibly up to 5.6 Gyr, according to Wright (2004)'s result. On the other hand, isochrone ages are more precise for stars that have evolved significantly away from the ZAMS, up to 17 Gyr (e.g. Nördstrom et al. 2004). In this manner chromospheric and isochrone techniques are complementary age estimator methods (Gustafsson 1999; Lachaume et al. 1999; Feltzing et al. 2001; Nördstrom et al. 2004).

The lithium method gives ages for only 20 of the EH stars, while the ages derived from the metallicity technique are upper limits. The currently available calibrations have bias against the older and younger stars, respectively. In this sense they might also be considered complementary. These two methods have greater uncertainties than the chromospheric or isochrone methods (e.g. Gustafsson 1999; Lachaume et al. 1999; Nördstrom et al. 2004) when applied to derive individual stellar ages. Thus, the chromospheric and the isochrone techniques seem to be the most reliable age indicators. In the case of the chromospheric technique, the D93 calibration produces, in general, results in better agreement with the isochrone technique than the RPM98 relation.

4.6. Limitations of the different age estimators

In this section we briefly comment on the applicability of the different age estimators employed to derive ages for the EH stars, and discuss systematic bias due to the use of these methods.

Chromospheric age determinations are based on the chromospheric activity of F, G and K stars. It is well established that the level emission decreases with time. However, at the present time is not clear up to what age this indicator can provide reliable stellar ages. Wright (2004) finds that the activity-age relation breaks down for ages $\gtrsim 5.6$ Gyr while Pace & Pasquini (2004) determine an earlier limit, of ~ 2 Gyr. Nonetheless,

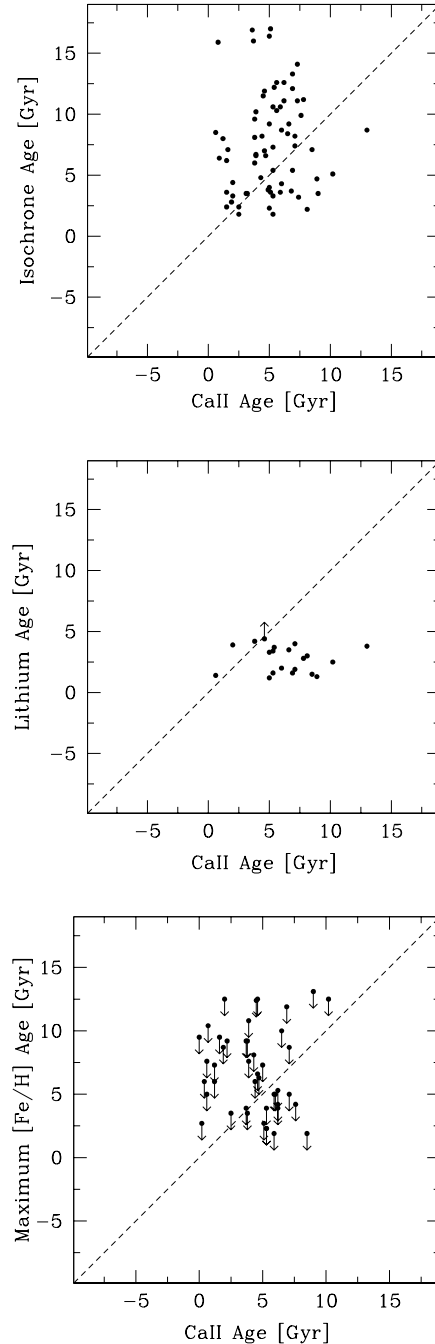


Fig. 6. Chromospheric ages against isochrone and lithium ages, and [Fe/H] upper limits, respectively.

this relation has been used well beyond the 5.6 Gyr limit (see, for example Henry et al. 1997; Donahue 1998; Wright et al. 2004). In any event, this method is more appropriate for the younger ages, when the level of stellar activity is sufficiently high. After this, the relation breaks down and enters into a plateau, offering little or no practical use as an age indicator. The uncertainty in the ages derived by this method depends on the temporal base line of observation of each individual star (see, for example, Henry et al. 2000a). Gustafsson (1999) esti-

mated a general uncertainty of about 30% in the chromospheric age derivations.

Isochrone ages strongly depend on the uncertainties of the observables (T_{eff} , M_V , and metallicity). In general the precision of these ages strongly varies with the position of the star on the HR diagram (see, for example, Nördstrom et al. 2004). For example, for low mass objects the isochrone traces tend to converge on this diagram (Pont & Eyer 2004). In addition, isochrone ages are less reliable for younger objects. On the other hand, this technique provides relatively more precise ages for stars that have evolved away from the ZAMS (Feltzing et al. 2001; Lachaume et al. 1999; Nördstrom et al. 2004). Recently, Pont & Eyer (2004) have extensively discussed this issue and proposed a method to estimate more accurate ages based on the Bayesian probability. Lachaume et al. (1999) and Nördstrom et al. (2004) have suggested typical uncertainties of about 50% in the ages derived by the isochrone technique.

Error estimations for isochrone and chromospheric ages are, in general, relatively large, 30–50%. Figure 6 shows relatively large dispersions, particularly in the case of the isochrone and chromospheric ages. This plot is probably reflecting the uncertainties in both techniques and not a peculiarity of the EH sample (see also Figure 8).

The $[\text{Fe}/\text{H}]$ -age relation has a large dispersion (Edvardsson et al. 1993; Carraro et al. 1998), although Pont & Eyer (2004) have significantly decreased this scattering. In addition, currently available calibrations do not include metal-rich objects, introducing a strong selection effect against (the younger) EH stars. The Li-age calibration is poorly constrained (Soderblom 1983; Pasquini et al. 1997, 1994; Boesgaard 1991) and biased toward younger objects. Consequently the ages derived by these methods suffer from large uncertainties. In spite of this, they are useful as independent age estimators.

The kinematic technique can be applied to estimate the ages for groups of stars and not to obtain individual stellar ages (Reid 2002). In addition, as the EH sample lies to the right of Parenago’s discontinuity in the velocity dispersion ($B-V$) diagram (see Figure 4), where old as well as young stars can be found. In any event, the kinematic ages of the EH stars are convenient for comparison with other groups of objects.

5. Comparison with the Solar Neighborhood stellar ages

To compare the ages of the EH sample with those of stars in the Solar Neighborhood with similar physical properties we selected three groups of nearby objects. Santos et al. (2001, 2005) provided a group of 94 F–G–K stars with no exoplanets detected by the Doppler technique; 31 of these stars have isochrone ages derived by Nördstrom et al. (2004). Sample A is composed of these 31 stars. Sample B contains 8684 F–G objects with distances between 3 and 238 pc taken from Nördstrom et al. (2004). Sample C has 1003 F–G single stars within the same range of distances as sample B, and snapshot (or instantaneous) values of $\text{Log } R'_{\text{HK}}$ derived by Henry et al.

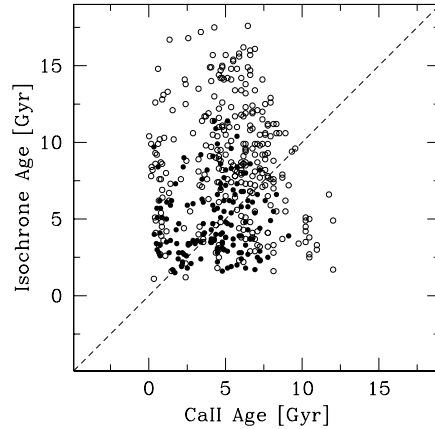


Fig. 8. Chromospheric ages vs isochrone ages for F and G-type solar neighborhood stars. Filled and empty circles correspond to F and G spectral types, respectively. Isochrone ages are taken from Nördstrom et al. (2004) and chromospheric determinations from Henry et al. (1996) and Strassmeier et al. (2000).

(1996) and Strassmeier et al. (2000). Isochrone ages for samples A and B were obtained from Nördstrom et al. (2004). Chromospheric ages for sample C were derived by Henry et al. (1996) and Strassmeier et al. (2000) applying the D93 calibration. We include only chromospheric and isochrone ages in our comparison as these are the most reliable estimators (see Section 4.5). In addition, we apply both methods for all stars independently of the ranges more appropriate for each of them, as also mentioned in Section 4.5., to avoid systematic effects.

In particular the 2 Gyr limit of Pace & Pasquini (2004) for the applicability of the chromospheric activity-age relation would introduce a strong bias toward younger ages, similar to the Li technique, with only $\sim 15\%$ of the EH sample within this limit. In this case the only meaningful comparison with the solar neighborhood would be of isochrone ages.

Figure 7 shows the isochrone age distributions for samples A and B and the chromospheric age distribution for sample C. In the cases of samples B and C the dashed and empty histograms correspond to G and F spectral types, respectively. We have cross-correlated samples B and C and plotted the result in Figure 8. A systematic effect is apparent in this figure. Isochrone ages are, on average, larger (older) than chromospheric ages for the Solar Neighborhood. This trend has already been seen in Figure 6 for the EH sample. We note that this systematic offset between isochrone and chromospheric ages would also persist for the 2 Gyr limit of Pace & Pasquini (2004).

In Figure 9 isochrone and chromospheric age distributions for the EH group are shown by separating the sample in G and F stars. Table 9 gives the medians and the standard deviations of samples A, B, and C as well as the EH group. The isochrone technique gives different median ages for objects of spectral types F and G for the nearby and the EH groups. On the other hand, the chromospheric method does not discrimi-

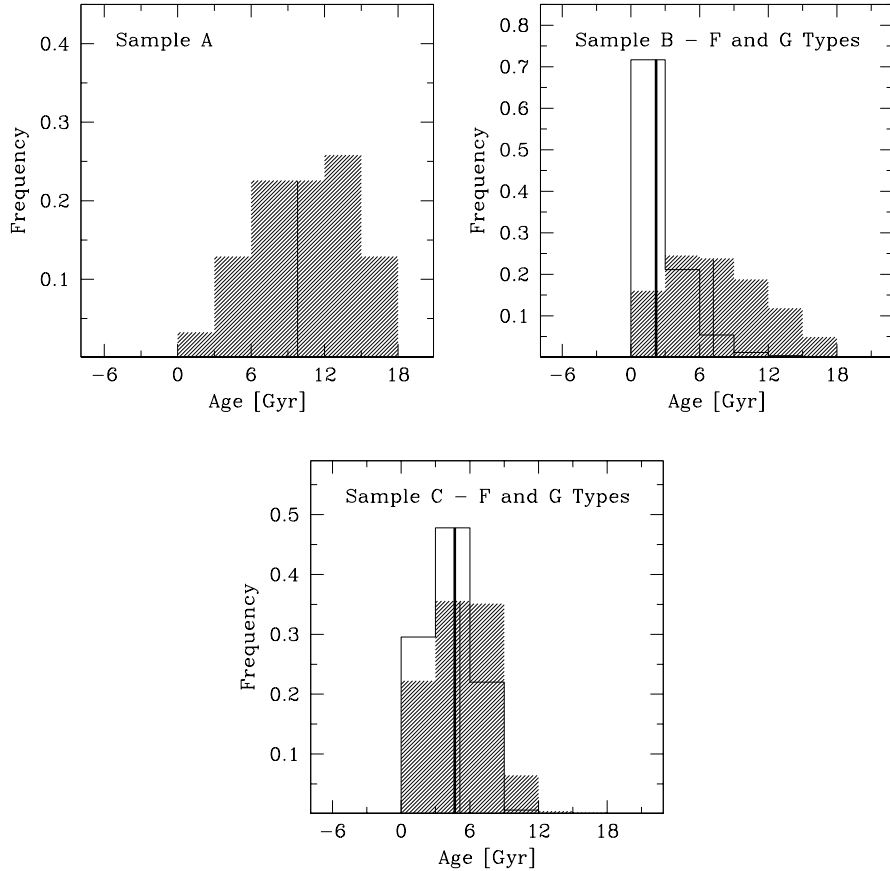


Fig. 7. Isochrone and chromospheric age distributions for the Solar Neighborhood stars. Isochrone ages for samples A and B were taken from Nördstrom et al. (2004). Chromospheric ages for sample C from Henry et al. (1996) and Strassmeier et al. (2000). Spectral types G and F in samples B and C are indicated by dashed and empty histograms, respectively. The vertical continuous lines show the median positions of each histogram. The thicker lines correspond to the F type and the lighter to the G type.

nate by spectral type. The median isochrone age for the (G and F) EH stars are ~ 1 – 2 Gyr larger (older) than for G and F stars in the solar neighborhood group. However the dispersions are large, ~ 2 – 4 Gyr.

The median age of G-type stars in sample A, 10.8 Gyr (25 objects, $\sigma = 3.4$ Gyr), and the median age of the same spectral type stars in the EH group, 8.2 Gyr (isochrone ages), are larger (older) than the median isochrone age for G-type stars in sample B, 7.2 Gyr (see Table 9). This is probably reflecting the fact that stars with high precision radial velocity measurements are selected among the less chromospherically active and thus, on average, are relatively older objects whereas sample B includes both active and inactive stars. We note, however, that the age dispersions for the three groups are large, including young and old objects in all cases.

Beichman et al. (2005) searched for infrared excesses in 26 FGK EH stars. These excess emissions are usually attributed to the presence of a debris disk surrounding the central star. Whereas none of the objects show excess at $24 \mu\text{m}$, 6 of them do have excess at $70 \mu\text{m}$. These authors, among other analysis, compared the chromospheric ages (obtained from Wright et al.

2004) for the stars with planets with those of nearby stars not associated with radial velocity detected planetary companions. They derived median ages of 6 and 4 Gyr for the samples of stars with and without exoplanets, although they considered this difference not statistically significant. It is interesting to note that we find a similar trend, with the EH stars being 1–2 Gyr older than the nearby stars. This result is based, however, on the isochrone ages.

We applied the KS to compare the distributions in Figure 7 with the EH histogram in Figure 9. Table 10 shows the results. The isochrone age distributions for F type stars in sample B and in the EH group are different, whereas for G type stars the distributions are more similar. With respect to the chromospheric ages, stars of F and G types in sample C and in the EH group show quite similar distributions.

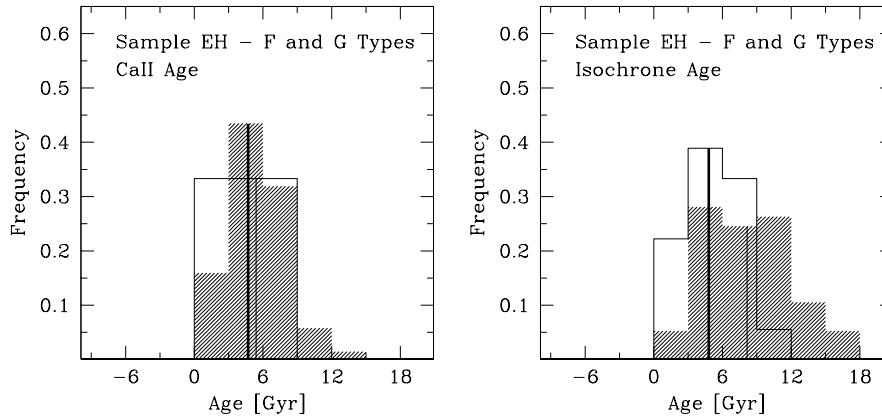
Figure 10 shows the EH group and sample B indicating stars of spectral types G and F in the left and right panels, respectively. The dashed histogram corresponds to the EH distribution and the empty histogram to sample B. In this figure, the apparent age difference between EH stars and sample B stars, is more evident for F spectral types. This is also sup-

Table 9. Median ages for the EH and Solar Neighborhood stars

Sample	Isochrone Median [Gyr]	Isochrone σ [Gyr]	Isochrone N	Chromospheric Median [Gyr]	Chromospheric σ [Gyr]	Chromospheric N
Sample A	9.8	3.6	31			
Sample B	2.8	3.7	8684			
F-type in Sample B	2.2	2.0	5357			
G-type in Sample B	7.2	4.1	2450			
Sample C				4.9	2.7	609
F-type in Sample C				4.7	2.1	159
G-type in Sample C				5.1	2.8	450
EH sample	7.4	4.2	79	5.2	4.2	112
F-type in EH sample	4.8	2.6	18	4.7	2.4	15
G-type in EH sample	8.2	3.8	57	5.4	3.5	69

Table 10. KS statistical test results for the EH and the Solar Neighborhood stars

	Isochrones ages KS test [%]	Chromospheric ages KS test [%]
EHS vs Sample A	0.92	
EHS vs Sample B - F type only	5.3×10^{-3}	
EHS vs Sample B - G type only	50.4	
EHS vs Sample C - F type only		13.0
EHS vs Sample C - G type only		3.1×10^{-5}

**Fig. 9.** Chromospheric and isochrone age distributions of EH stars. Spectral types G and F are indicated by dashed and empty histograms, respectively. The vertical continuous lines show the median positions of each histogram. The thicker lines correspond to the F type and the lighter to the G type.

ported by the KS test result in Table 10. A similar comparison for the chromospheric ages is meaningless as this method does not discriminate by spectral types.

6. Correlations of the stellar properties with age

We searched for correlations between the EH stellar properties and age. In Figure 11, upper panels, we plotted L_{IR}/L_{\odot} , the excess over the stellar luminosity, vs chromospheric and isochrone ages. The luminosity ratios were obtained from Saffe & Gomez (2004). In the lower panels of the same figure we show $[\text{Fe}/\text{H}]$ vs age. Whereas no correlation is apparent

with the excess over the stellar luminosity, a weak correlation shows up with the $[\text{Fe}/\text{H}]$. In other words, the metallicity dispersion seems to increase with age.

To verify whether this is a real tendency, we divided the EH sample in two bins, adopting $\text{Log Age} = 0.5$ as the cut point for the CaII ages and $\text{Log Age} = 0.75$ for the isochrone ages, to have more even sub-samples in both cases. We then calculated the rms corresponding to the average age in each bin. For the CaII ages (lower left panel in Figure 11), we obtained for Log Age greater and less than 0.5, an rms of 0.16 and 0.21 dex, respectively. In the case of the isochrone ages (lower right panel in Figure 11), we derived the same rms for stars with Log Age

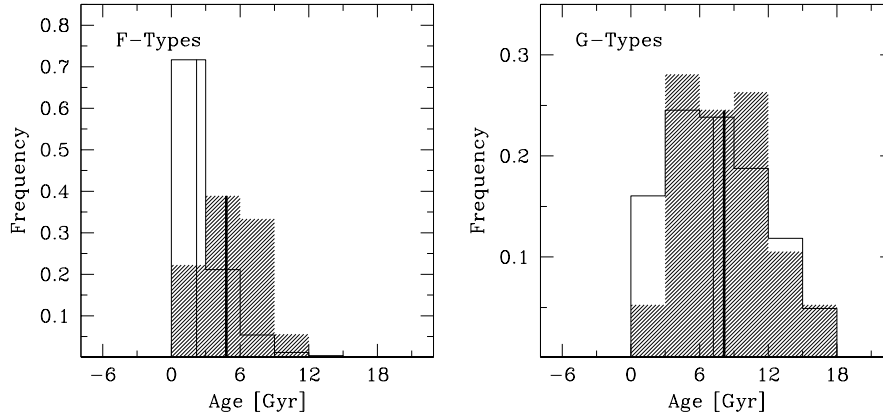


Fig. 10. Isochrone age distributions for EH stars (shade histograms) and sample B (empty histograms). The right panel corresponds to stars of spectral type F in both samples and the left panel to G-type objects. The vertical continuous lines show the median positions of each histogram. The thicker lines correspond to the F type and the lighter to the G type.

in the first and second bin. We repeated this analysis adopting chromospheric ages for the EH stars with $\text{Log } R'_{\text{HK}} < -5.1$ and isochrone ages for the rest of the objects. No substantial change is observed in Figure 11.

Beichman et al. (2005) found little or no correlation of the $70 \mu\text{m}$ excess with the (chromospheric) age, metallicity and spectral type of 6 EH stars. Nevertheless their analysis suggests that the frequency of excess at $70 \mu\text{m}$ in stars with planets is at least as large as for typical Vega-like candidate objects selected by IRAS (Plets & Vynckier 1999). This result is somehow different to the finding of Greaves et al. (2004) based on sub-mm observations of 8 EH stars (Beichman et al. 2005).

7. Summary

We measured the chromospheric activity in a sample of 49 EH stars, observable from the southern hemisphere. Combining our data with those from the literature we derived the chromospheric activity index, R'_{HK} , and estimated ages for the complete EH stars sample with chromospheric data (112 objects), adopting the D93 calibration. We applied other methods to estimate ages, such as: Isochrone, lithium and metallicity abundances and space velocity dispersions, to compare with the chromospheric results.

The derived median ages for the EH group are 5.2 and 7.4 Gyr, using chromospheric and isochrone methods, respectively. However, the dispersions in both cases are rather large, about ~ 4 Gyr. In the derivation of the median chromospheric age we have applied the chromospheric activity-age relation beyond the 2 and 5.6 Gyr suggested by Pace & Pasquini (2004) and Wright (2004), respectively. In particular the first limit would indicate that the isochrone technique is, in practice, the only tool currently available to derive ages for the complete sample of the EH stars.

Lithium ages and metallicity upper limits are only available for a subset of the EH stars, as the corresponding calibrations do not cover the complete range of Li and [Fe/H] abundances

of this type of objects. This fact precludes any statistical application of these ages for the EH stars. The kinematic technique does not provide individual stellar ages. In addition, kinematic ages are less reliable because most EH stars lie to the right of Parenago's discontinuity.

The median ages for the G and F EH stars derived from the isochrone method are $\sim 1-2$ Gyr larger (older) than the median ages for G and F solar neighborhood stars. We caution, however, that the dispersions in both distributions are large, $\sim 2-4$ Gyr. The EH stars, analyzed here, have been selected by means of the Doppler technique that favors the detection of planetary-mass companions around the less chromospherically active and slower rotator stars, where radial velocity measurements can reach high precisions of \lesssim few m/s (see, for example, Henry et al. 1997; Vogt et al. 2000; Pepe et al. 2002). As the chromospheric activity and the rotation decrease with age, on average, we may expect the EH stars be older than stars with similar physical properties not known to be associated with planets. The later group of objects is likely to include a significant fraction of the more chromospherically active and thus younger stars for which high precision in radial velocity measurements are difficult to achieve.

With regard to the F EH stars, our result may suggest that these objects are older than F nearby stars not known to be associated with planets in opposition to Suchkov & Schultz (2001)'s result. However, the relatively large dispersion in our ages and the rather poor number of stars analyzed by Suchkov & Schultz (2001) render this apparent discrepancy meaningless. We searched for correlations between the age, the L_{IR}/L_* and the metallicity. No clear tendency is found in the first case, whereas the metallicity dispersion seems to slightly increase with age.

Acknowledgements. This research has made use of the SIMBAD database, operated at CDS, Strasbourg, France. An anonymous referee provided helpful comments and suggestions that improved both the content and the presentation of this article.

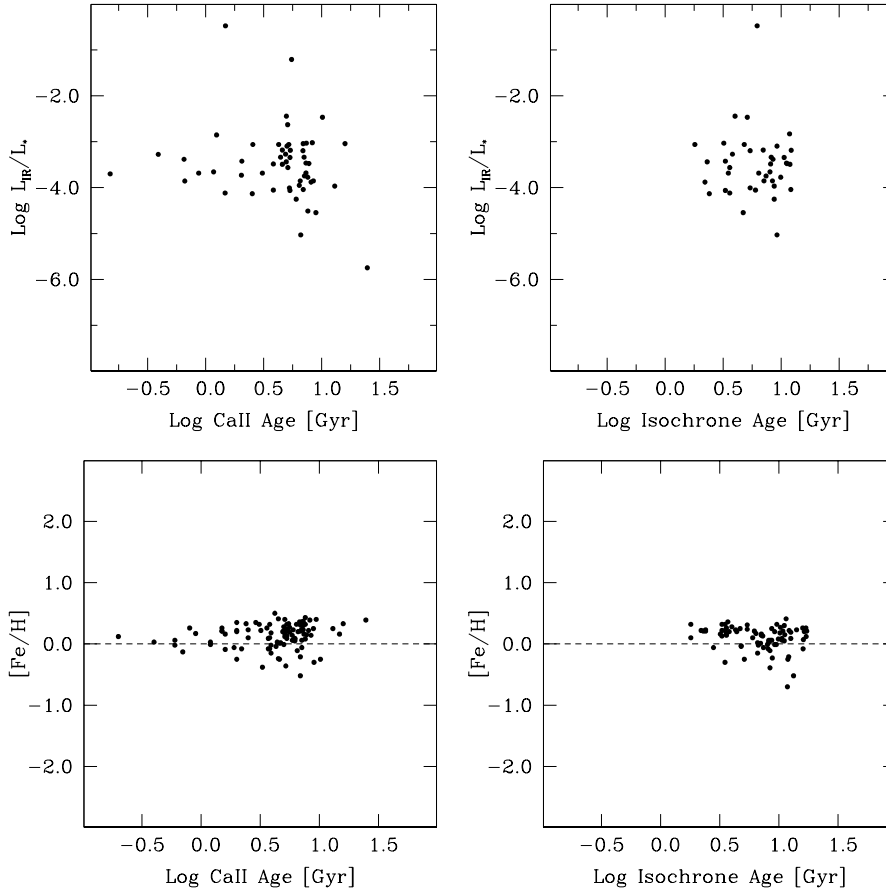


Fig. 11. Upper panels: L_{IR}/L_* vs chromospheric and isochrone ages. Lower panel: $[\text{Fe}/\text{H}]$ vs chromospheric and isochrone ages.

References

- Baliunas, S. L., Hartmann, L., Noyes, R. W., Vaughan, H., Preston, G. W., Frazer, J., Lanning, H., Middelkoop, F., Mihalas, S., 1983, *ApJ* 275, 752
- Baliunas, S. L., Donahue, R. A., Soon, W. H., Horne, J. H., Frazer, J., Woodard-Eklund, L., Bradford, M., Rao, L. M., Wilson, O. C.; Zhang, Q.; and 17 coauthors, 1995a, *ApJ* 438, 269
- Baliunas S. L., Donahue S. A., Soon W., Guilliland R., Soderblom D., 1995b, *BAAS* 27, 839
- Baliunas, S., Sokoloff, D., Soon, W., 1996, *ApJ* 457, L99
- Barbieri, M., Gratton, R. G., 2002, *A&A* 384, 879
- Barry D. C., Cromwell R. H., Hege E. K., 1987, *ApJ* 315, 264
- Beichman, C. A., Bryden, G., Rieke, G. H., Stansberry, J. A., Trilling, D. E., Stapelfeldt, K. R., Werner, M. W., Engelbracht, C. W., Blaylock, M., Gordon, K. D., Chen, C. H., Su, K. Y. L., Hines, D. C., 2005, *ApJ* 622, 1160
- Binney, J. J., Dehnen, W., Bertelli, G., 2000, *MNRAS* 318, 658
- Boesgaard A. M., 1991, *ApJ* 370, 95
- Butler, R. P., Marcy, G. W., Fischer, D. A., Brown, T. M., Conantos, A. R., Korzennik, S. G., Nisenson, P., Noyes, R. W., 1999, *ApJ* 526, 916
- Butler, R. P., Marcy, G. W., Vogt, S. S., Apps, K., 1998, *PASP* 110, 1389
- Butler, R. P., Vogt, S. S., Marcy, G. W., Fischer, D. A., Henry, G. W., Apps, K., 2000, *ApJ* 545, 504
- Butler, R. P., Marcy, G. W., Vogt, S. S., Tinney, C. G., Jones, H. R. A., McCarthy, C., Penny, A. J., Apps, K., Carter, B., 2002, *ApJ* 578, 565
- Butler, R., Marcy, G. W., Vogt, S. S., Fischer, D. A., Henry, G. W., Laughlin, G., Wright, J. T., 2003, *ApJ* 582, 455
- Butler, R. P., Vogt, S. S., Marcy, G. W., Fischer, D. A., Wright, J. T., Henry, G. W., Laughlin, G., Lissauer, J. J., 2004, *ApJ* 617, 580
- Carraro, G., Ng, Y. K., Portinari, L., 1998, *MNRAS* 296, 1045
- Charbonneau, D., Brown, T. M., Latham, D. W., Mayor, M., 2000, *ApJ* 529L, 45
- Chen B., Asaiian R., Figueras F., Torra J., 1997, *A&A* 318, 29
- Cuntz M., Saar S. H., Musielak, Z. E., 2000, *ApJL* 533, 151
- Dehnen, W., Binney, J., 1998, *MNRAS* 298, 387
- Donahue R. A., 1993, Ph D Thesis, New Mexico State University
- Stellar Ages Using the Chromospheric Activity of Field Binary Stars, in *ASP Conf. Ser. 154, The Tenth Cambridge Workshop on Cool Stars, Stellar Systems and the Sun*, ed: R. Donahue & J. Bookbinder (San Francisco: ASP), CD-834, 1998

- Donahue, R. A., Saar, S. H., Baliunas, S. L., 1996, *ApJ* 466, 384
- Duncan, D. K., 1981, *ApJ* 248, 651
- Duncan, D. K., Vaughan, A. H., Wilson, O. C., Preston, G. W., Frazer, J., Lanning, H., Misch, A., Mueller, J., Soyumer, D., Woodard, L., Baliunas, S. L., 1991, *ApJS* 76, 383
- Durney, B. R., Mihalas, D., Robinson, R. D., 1981, *PASP* 93, 537
- Edvardsson, B., Andersen, J., Gustafsson, B., Lambert, D. L., Nissen, P. E., Tomkin, 1193, *A&A* 275, 101
- Eggen O. J., 1990, *PASP* 102, 166
- Feltzing, S., Holmberg, J., Hurley, J. R., 2001, *A&A* 377, 911
- Fischer, D. A., Marcy, G. W., Butler, R. P., Vogt, S. S., Apps, K., 1999, *PASP* 111, 50
- Fischer, D. A., Marcy, G. W., Butler, R. P., Vogt, S. S., Frink, S., Apps, K., 2001, *ApJ* 551, 1107
- Fischer, D. A., Marcy, G. W., Butler, R. P., Vogt, S. S., Walp, B., Apps, K., 2002, *PASP* 114, 529
- Fischer, D. A., Marcy, G. W., Butler, R. P., Laughlin, G., Vogt, S. S., 2002, *ApJ* 564, 1028
- Fischer, D. A., Laughlin, G., Butler, P., Marcy, G., Johnson, J., Henry, G., Valenti, J., Vogt, S., Ammons, M., Robinson, S., Spear, G., Strader, J., Driscoll, P., Fuller, A., Johnson, T., Manrao, E., McCarthy, C., Munoz, M., Tah, K. L.; Wright, J., Ida, S., Sato, B., Toyota, E., Minniti, D., 2005, *ApJ* 620, 481
- Girardi, L., Bressan, A., Bertelli, G., Chiosi, C., 2000, *A&AS* 141, 371
- Gonzalez, G., 1997, *MNRAS* 285, 403.
- Gonzalez, G., 1998, *A&A* 334, 221
- Gonzalez, G., 1999, *MNRAS* 308, 447
- Gonzalez, G., Laws, C., 2000, *ApJ* 119, 390
- Gonzalez, G., Laws, C., Tyagi, S., Reddy, B., 2001, *AJ* 121, 432.
- Greaves, J. S., Holland, W. S., Jayawardhana, R., Wyatt, M. C., Dent, W. R. F., 2004, *MNRAS*, 348, 1097
- Gustafsson, B., 1999, *ASP Conf. Ser.* 192, 91. Hybeny, Heap & Cornett eds.
- Hatzes, A. P., Cochran, W. D., Endl, M., McArthur, B., Paulson, D. B., Walker, G. A. H., Campbell, B., Yang, S., 2003, *ApJ* 599, 1383
- Henry, T., Soderblom, D., Donahue, R., Baliunas, S., 1996, *AJ* 111, 439.
- Henry, G. W., Baliunas, S. L., Donahue, R. A., Soon, W. H., Saar, S. H., 1997, *ApJ*, 474, 503
- Henry, G. W., Baliunas, S. L., Donahue, R. A. et al., 2000, *ApJ* 531, 415
- Henry, G. W., Marcy, G. W., Butler, R. P., Vogt, S. S., 2000, *ApJL* 529, 41
- Herbig, G. H., 1985, *ApJ* 289, 269
- Houk, N., 1978, *Catalogue of Two-Dimensional Spectral Types for the HD stars*, Vol. 2, Dept. of Astronomy, Univ. Michigan, Ann Arbor
- Houk, N., 1982, *Catalogue of Two-Dimensional Spectral Types for the HD stars*, Vol. 3, Dept. of Astronomy, Univ. Michigan, Ann Arbor
- Houk, N., Cowley, A. P., 1978, *Catalogue of Two-Dimensional Spectral Types for the HD stars*, Vol. 1, Dept. of Astronomy, Univ. Michigan, Ann Arbor
- Huovelin, J., Saar, S. H., Tuominen, I., 1988, *ApJ* 329, 882
- Ibukiyama, A.; Arimoto, N., 2002, *A&A* 394, 927
- Israelian, G., Santos, N. C., Mayor, M., Rebolo, R., 2004, *A&A* 414, 601
- Jones, H. R. A., Butler, R. P., Tinney, C. G., Marcy, G. W., Penny, A. J., McCarthy, C., Carter, B. D., 2003, *MNRAS* 341, 948
- Karatas, Y., Bilir, S., Schuster, W. J., 2005, *MNRAS* 360, 1345
- King, J. R., Villarreal, A. R., Soderblom, D. R., Gulliver, A. F., Adelman, S. J., 2003, *AJ* 125, 1980
- Lachaume R., Dominik C., Lanz T., Habing H. J., 1999, *A&A* 348, 897
- Laughlin, G., Adams, F. C., 1997, *ApJ* 491, 51
- Laws, C., Gonzalez, G., Walker, K. M., Tyagi, S., Dodsworth, J., Snider, K., Suntzeff, N. B., 2003, *AJ* 125, 2664
- Lovis C., Mayor M., Bouchy F., Pepe F., Queloz D., Santos N.C., Udry S., Benz W., Bertaux J.L., Mordasini C., Sivan J.P., 2005, arXiv:astro-ph/0503660
- Manoj, P., Bhatt, H. C., 2005, *A&A* 429, 525
- Marcy, G. W., Butler, R. P., Williams, E., Bildsten, L., Graham, J. R., Ghez, A. M., Jernigan, J. G., 1997, *ApJ* 481, 926
- Marcy, G. W., Butler, R. P., Vogt, S., Shirts, P., 1998, *AAS* 192, 801
- Marcy, G. W., Butler, R. P., Vogt, S. S., Fischer, D., Liu, M. C., 1999, *ApJ* 520, 239
- Marcy, G. W., Butler, R. P., Vogt, S. S., 2000, *ApJ* 536, L43
- Marcy, G. W., Butler, R. P., Vogt, S. S., Liu, M. C., Laughlin, G., Apps, K., Graham, J. R., Lloyd, J., Luhman, K. L., Jayawardhana, R., 2001, *ApJ* 555, 418
- Marcy, G., Butler, R., Fischer, D. A., Laughlin, G., Vogt, S. S., Henry, G.W., Pourbaix, D., 2002, *ApJ* 581, 1375
- Mayor, M., Queloz, D., 1995, *Nature* 378, 355
- Mayor, M., Pepe, F., Queloz, D., Bouchy, F., Rupprecht, G., Lo Curto, G., Avila, G., Benz, W., Bertaux, J.-L., Bonfils, X., and 22 coauthors, 2003, *Msngr* 114, 20
- Mayor, M., Udry, S., Naef, D., Pepe, F., Queloz, D., Santos, N. C., Burnet, M., 2004, *A&A* 415, 391
- Middelkoop, F., 1982, *A&A* 113, 1
- Middelkoop, F., Vaughan, A. H., Preston, G. W., 1981, *A&A* 96, 401
- Montes, D., Martin, E. L., 1998, *A&AS* 128, 485
- Montes, D., Ramsey, L. W., Welty, A. D., 1999, *ApJS* 123, 283
- Montes, D., Martin, E. L., Fernandez-Figueroa, M. J., Cornide, M., de Castro, E., 1997, *A&AS* 123, 473
- Montesinos, B., Fernandez-Figueroa, M. J., de Castro, E., 1987, *MNRAS* 229, 627
- Naef, D., Mayor, M., Pepe, F., Queloz, D., Santos, N. C., Udry, S., Burnet, M., 2001, *A&A* 375, 205
- Ng, Y. K., Bertelli, G., 1998, *A&A* 329, 943
- Nordstrom, B., Mayor, M., Andersen, J., Holmberg, J., Pont, F., Jorgensen, B. R., Olsen, E. H., Udry, S., Mowlavi, N., 2004, *A&A* 418, 989

- Noyes, R. W., Hartmann, L. W., Baliunas, S. L., Duncan, D. K., Vaughan, A. H., 1984, *ApJ* 279, 763
- Pace, G., Pasquini, L., 2004, *A&A* 426, 1021
- Parento, P. P., 1950, *AZh* 27, 150
- Pasquini, L., Liu, Q., Pallavicini, R., 1994, *A&A* 287, 191
- Pasquini, L., Randich, S., Pallavicini, R., 1997, *A&A* 325, 535
- Paulson, D. B., Saar, S. H., Cochran, W. D., Hatzes, A. P., 2002, *AJ* 124, 572
- Paulson, D. B., Cochran, W. D., Hatzes, A. P., 2004, *AJ* 127, 3579
- Pepe, F., Mayor, M., Galland, F., Naef, D., Queloz, D., Santos, N. C., Udry, S., Burnet, M., 2002, *A&A* 388, 632
- Pepe, F., Mayor, M., Queloz, D., Benz, W., Bonfils, X., Bouchy, F., Curto, G. Lo, Lovis, C., Mégevand, D., Moutou, C., Naef, D., Rupprecht, G., Santos, N. C., Sivan, J.-P., Sosnowska, D., Udry, S., 2004, *A&A* 423, 385
- Plets, H., & Vynckier, C., 1999, *A&A* 343, 496
- Pont F., Eyer L., 2004, *MNRAS* 351, 487
- Press W. H., Teukolsky S. A., Vetterling W. T., Flannery B. P., 1992, *Numerical Recipes in Fortran: The Art of Scientific Computing*, Cambridge University Press, 2nd edition, p. 617
- Queloz, D., Mayor, M., Weber, L., Blcha, A., Burnet, M., Confino, B., Naef, D., Pepe, F., Santos, N., Udry, S., 2000, *A&A* 354, 99
- Queloz, D., Henry, G. W., Sivan, J. P., Baliunas, S. L., Beuzit, J. L., Donahue, R. A., Mayor, M., Naef, D., Perrier, C., Udry, S., 2001, *A&A* 379, 279
- Reddy, B. E., Tomkin, J., Lambert, D. L., Allende Prieto, C., 2003, *MNRAS* 340, 304
- Reid, N., 2002, *PASP* 114, 306.
- Rocha-Pinto, H., Maciel, W., 1998, *MNRAS* 298, 332.
- Rocha-Pinto, H. J., Maciel, W. J., Scalo, J., Flynn, C., 2000, *A&A* 358, 850
- Roman, N. G., 1954, *AJ* 59, 307
- Rubenstein, E. P., Shaefer, B. E., 2000, *ApJ* 529, 1031
- Ryan, S., 2000, *MNRAS* 316, L35
- Skumanich A., 1972, *ApJ* 171, 565
- Saar S.H., Cuntz M., 2001, *MNRAS* 325, 55
- Saar S.H., Donahue, R. A., 1997, *ApJ* 485, 319
- Saar, S. H., Osten, R. A., 1997, *MNRAS* 284, 803
- Saar S.H., Butler R.P., Marcy G.w. 1998, *ApJL* 498, 153
- Saffe C., Gomez M., 2004, *A&A* 423, 221
- Salasnich, B., Girardi, L., Weiss, A., Chiosi, C., 2000, *A&A* 361, 1023
- Santos N. C., Israelian G., Mayor M., 2000, *A&A* 363, 228
- Santos, N. C., Mayor, M., Naef, D., Pepe, F., Queloz, D., Udry, S., Blecha, A., 2000, *A&A* 361, 265
- Santos N. C., Israelian G., Mayor M., 2001, *A&A* 373, 1019
- Santos, N. C., Mayor, M., Naef, D., Pepe, F., Queloz, D., Udry, S., Burnet, M., Clausen, J. V., Helt, B. E., Olsen, E. H., Pritchard, J. D., 2002, *A&A* 392, 215
- Santos, N. C., Udry, S., Mayor, M., Naef, D., Pepe, F., Queloz, D., Burki, G., Cramer, N., Nicolet, B., 2003, *A&A* 406, 373
- Santos, N. C., Israelian, G., Mayor, M., Rebolo, R., Udry, S., 2003, *A&A* 398, 363
- Santos, N. C., Bouchy, F., Mayor, M., Pepe, F., Queloz, D., Udry, S., Lovis, C., Bazot, M., Benz, W., Bertaux, J.-L., Lo Curto, G., Delfosse, X., Mordasini, C., Naef, D., Sivan, J.-P., Vauclair, S., 2004, *A&AL* 426, 19
- Santos, N. C., Israelian, G., Mayor, M., 2004, *A&A* 415, 1153
- Santos, N. C., Israelian G., Mayor, M., Bento, J.P., Almeida, P. C., Sousa, S. G., Ecuivillon, A., 2005, *astro-ph/0504154*
- Shkolnik, E., Walker, G. A. H., Bohlender, D. A., 2003, *ApJ* 597, 1092
- Shkolnik, E., Walker, G. A. H., Bohlender, D. A., Gu, P.-G., Kürster, M., 2004, *AAS* 205, 1123
- Soderblom, D. R., 1983, *ApJS* 53, 1
- Soderblom, D. R., 1985, *AJ* 90, 2103
- Soderblom, D. R., Clements, S. D., 1987, *AJ* 93, 920
- Soderblom, D. R., Mayor, M., 1993, *ApJ* 402, L5
- Soderblom, D. R., Duncan, D., Johnson, D., 1991, *ApJ* 375, 722.
- Soderblom, D. R., Stauffer, J. R., Hudon, J. D., Jones, B. F., 1993, *ApJS* 85, 315
- Sozzetti, A., Yong, D., Torres, G., Charbonneau, D., Latham, D. W., Allende Prieto, C., Brown, T. M., Carney, B. W., Laird, J. B., 2004, *ApJL* 616, 167
- Strassmeier, K. G., Fekel, F. C., Bopp, B. W., Dempsey, R. C., Henry, G. W., 1990, *ApJS* 72, 191
- Strassmeier, K., Washuettl, A., Granzer, Th., Scheck, M., Weber, M., 2000, *A&AS* 142, 275
- Suchkov, A. A., Schultz, A. B., 2001, *ApJL* 549, 237
- Tinney, C. G., McCarthy, C., Jones, H. R. A., Butler, R. P., Carter, B. D., Marcy, G. W., Penny, A. J., 2002, *MNRAS* 332, 759
- Tinney, C. G., Butler, R. P., Marcy, G. W., Jones, H. R. A., Penny, A. J., Vogt, S. S., Apps, K., Henry, G. W., 2002, *ApJ* 551, 507
- Twarog, B. A., 1980, *ApJ* 242, 242
- Udry, S., Mayor, M., Naef, D., Pepe, F., Queloz, D., Santos, N. C., Burnet, M., Confino, B., Melo, C., 2000, *A&A* 356, 590
- Udry, S., Mayor, M., Naef, D., Pepe, F., Queloz, D., Santos, N. C., Burnet, M., 2002, *A&A* 390, 267
- Udry, S., Eggenberger, A., Mayor, M., Mazeh, T., Zucker, S., 2004, *RMxAC* 21, 207
- Vaughan, A. H., Preston G. W., 1980, *PASP* 92, 385
- Vaughan, A. H., Preston, G. W., Baliunas, S. L., Hartmann, L. W., Noyes, R. W., Middelkoop, F., Mihalas, D., 1981, *ApJ* 250, 276
- Vaughan, A. H., Preston, G. W., Wilson, O. C., 1978, *PASP* 90, 267
- Vogt, S. S., Marcy, G. W., Butler, R. P., Apps, K., 2000, *ApJ* 536, 902
- Vogt, S. S., Butler, R. P., Marcy, G. W., Fischer, D. A., Pourbaix, D., Apps, K., Laughlin, G., 2002, *ApJ* 568, 352
- Walker, G. A. H., Bohlender, D. A., Walker, A. R., Irwin, A. W., Yang, S. L. S., Larson, A., 1992, *ApJL* 396, 91
- Wielen, R., Fuchs, B., Dettbarn, C., 1996, *A&A* 314, 438
- Wilson, O., 1963, *ApJ* 138, 832.
- Wilson, O. C., 1970, *ApJ* 160, 255
- Wright, J. T., 2004, *AJ* 128, 1273

- Wright, J. T., Marcy, G. W., Butler R. P., Vogt, S. S., 2004,
ApJS 152, 261
- Young, A., Ajir, F., Thurman, G., 1989, PASP 101, 1017
- Zucker, S., Mazeh, T., Santos, N. C., Udry, S., Mayor, M.,
2004, A&A 426, 695
- Zuckerman B., 2001, ARA&A 39, 549.